GUIDANCE OF AN AEROMANEUVERING ORBIT-TO-ORBIT SHUTTLE THROUGH A STATISTICALLY VARYING ATMOSPHERE

By

John Joseph Rehder (NASA Langley)

Bachelor of Aerospace Engineering
Georgia Institute of Technology
March 1970

A Thesis Submitted to the
Faculty of
The School of Engineering and Applied Science
of the George Washington University
in partial satisfaction of the requirements
for the degree of Master of Science

June 1975

Thesis Directed by
Dr. Terry A. Straeter

ABSTRACT

One candidate for a reusable upper stage to be carried by the Space Shuttle is an Aeromaneuvering Orbit-to-Orbit Shuttle (AMOOS). This concept uses the drag of the vehicle during a pass through the atmosphere rather than the propulsion system to slow the vehicle on a return from a high energy orbit. In this paper, the nature and magnitude of the sensitivity of AMOOS to uncertainties in the properties of the atmosphere is shown. Various guidance schemes for correcting for the effects that the unpredictable variations in the atmosphere have on the trajectory are discussed. For the mission studied here, a payload retrieval from geosynchronous orbit with aerodynamic plane change, a linear feedback guidance scheme was developed. A relatively simple heuristic law was used to demonstrate the concept. Using optimal control theory a feedback law was developed analytically. Testing with a large number of different atmospheres showed this law to be a feasible means of controlling the AMOOS trajectory. Also, refinements to the technique offer promise of significant improvement and these are discussed.

TABLE OF CONTENTS

INTRODUCTION

One essential element of the Space Transportation being developed for future space operations is the reusable upper stage to be carried by the Space Shuttle. The current baseline vehicle is a purely propulsive Orbit-to-Orbit Shuttle (OOS). An alternative candidate, the Aeromaneuvering Orbit-to-Orbit Shuttle (AMOOS), uses the drag of the vehicle during a pass through the atmosphere rather than the propulsion system to slow the vehicle on a return from high orbit. AMOOS offers much more payload capability than OOS and uses current rather than advanced technology.

One of the key problem areas of AMOOS is its sensitivity to uncertainties in atmospheric properties and the development of a guidance law which will correct for these uncertainties and insure that the vehicle flies the desired trajectory. This paper will describe the background of the AMOOS concept, compare it with the conventional OOS, and examine the guidance problem. The nature and the magnitude of the sensitivity of AMOOS to the state of the atmosphere will be discussed. This sensitivity was determined by linking a trajectory program with an atmosphere generator program which produces a large number of different atmospheres that statistically match actual atmosphere data. The data from a large number of trajectories provided clues for possible guidance schemes which use the aerodynamic capability of the vehicle.

In particular, a linear feedback guidance law will be developed and tested on a large number of different atmospheres. First, a simple

heuristic law will be used to demonstrate the feedback technique. Then, using optimal control theory, a feedback law will be developed analytically. Possible refinements to the technique and areas of further study will also be proposed.

NOMENCLATURE

A	Jacobian matrix of F with respect to $\overline{X}$, $\frac{\partial \overline{F}}{\partial X}$
B	Jacobian matrix of F with respect to $\overline{U}$, $\frac{\partial \overline{F}}{\partial U}$
C	Control gain matrix
C_L	Lift coefficient
C_D	Drag coefficient
D	Observaibility matrix
E	Energy, m^2/s^2
$\overline{F}$	Force matrix in physical system
H	Hamiltonian
J	Performance index
k	Gain in heuristic feedback law
L/D	Lift-to-drag ratio
m	Meter
Q	State deviation matrix multiplier
R	Control deviation matrix multiplier
r	Magnitude of position vector, m
S	Terminal condition matrix multiplier
s	Second
t	time, s
$\overline{U}$	Control vector
$\overline{u}$	perturbation of control vector, δU
V	Magnitude of velocity vector, m/s

V_1, V_2, V_3	Components of velocity vector, m/s
$\overline{X}$	State vector
$\overline{x}$	Perturbation of state vector, $\delta\overline{X}$
μ	Gravitational constant, m^3/s^2
ϕ	Bank angle, deg.

ABBREVIATIONS

OOS	Orbit-to-Orbit Shuttle
AMOOS	Aeromaneuvering Orbit-to-Orbit Shuttle
POST	Program to Optimize Simulated Trajectories

BACKGROUND

To fully realize the potential of the Space Shuttle presently being developed under the direction of NASA, a reusable upper stage, or Orbit-to-Orbit Shuttle (OOS), becomes a necessary component of the total space transportation system. The OOS, placed in orbit by the Shuttle, would deliver and retrieve payloads from high energy orbits. Detailed studies of a purely propulsive OOS are presently underway using a baseline vehicle described in reference 1. The mission profile for such a vehicle and a schematic of its configuration are shown in figures 1 and 2. The maximum weight of the OOS is constrained by the maximum Shuttle payload capability of 29484 kg. With this restriction, even technology advances such as composite materials and a new improved propulsion system will not give OOS the capability to perform all of the missions proposed in the payload mission model without the use of multiple Shuttle launches. One study (ref. 2) states that a significant number of missions will require two Shuttle/OOS launches, thus increasing the cost and complexity of those missions. This situation is further aggravated by the high sensitivity of the performance of a purely propulsive OOS to changes in inert weight and engine specific impulse. One possible way to reduce this sensitivity and increase payload capability of a reusable upper stage may be to use the atmospheric forces rather than the engine thrust to brake the vehicle during the transfer from high orbit to Shuttle rendezvous altitude. This could eliminate about 1/4 of the propulsive ΔV required for a round trip geosynchronous mission.

The concept of using the atmosphere to alter a vehicle's orbit has been the subject of much study in the past. Most of this work has been in the form of analytical studies of synergetic plane change, which uses a combination of propulsive and aerodynamic forces to change the inclination of the vehicle's orbital plane (refs. 3-12). The initial and final orbits of the vehicle are essentially the same except for inclination. These studies, limited to near earth orbit, indicate that the synergetic plane change can give substantial fuel savings for vehicles with hypersonic L/D more than 2.

The technique of using the atmosphere to slow an orbital vehicle has been in use since the early days of space flight. However, aerobraking, as applied to full reentry from space requires that essentially all of vehicle's energy be dissipated, while the application to a return to a low earth orbit from synchronous orbit requires only a specific, precise amount of energy loss.

In recent years, several studies have investigated the potential of aerobraking for OOS type vehicles. Multi-pass trajectories were considered to minimize aerodynamic heating. Guidance and heating constraints were determined (ref. 13) and an analytical technique for calculating some trajectory parameters was developed (ref. 14) for multipass missions. The trajectory of a typical aerobraking mission is illustrated in figure 3. A later comprehensive study investigated the feasibility and practicality of the aerobraking mode for return from high orbit of an OOS with an aerobraking kit attached (ref. 15). Some of the conclusions of this

study were that the aerobraking mode was feasible, payload was maximized by missions with 25 to 35 aerobraking passes, and that, contrary to conventional OOS, the aerobraking OOS could perform the baseline round trip mission using current technology.

The most recent activity in this area has been a feasibility study of a new vehicle called the Aeromaneuvering Orbit-to-Orbit Shuttle (AMOOS) (refs. 16, 17). The results of this study include the identification of the most promising configurations for AMOOS, demonstration of potentially large payload gains, and identification of problem areas. One critical problem area was the sensitivity of AMOOS to uncertainties in the properties, particularly density, of the atmosphere and the guidance of AMOOS through an unpredictable atmosphere. This problem and its solution is the subject of this paper.

AMOOS

The vehicle used in the present investigation was derived in the AMOOS feasibility studies. This section provides a general description of AMOOS and the particular configuration studied herein using material from references 16 and 17.

The AMOOS mission will differ from that of the propulsive OOS only in the manner in which it achieves a phasing orbit with the Shuttle during the return phase. AMOOS will be targeted to enter the earth's atmosphere for a prescribed number of passes. It will exit after the last pass with just enough velocity to carry it to phasing orbit apogee. At apogee, a short burn is required to achieve phasing orbit perigee. Once this is done, the AMOOS mission is then identical to that of the propulsive OOS.

The most promising configuration evolved as a compromise between high lift to maximize control authority, high drag to minimize TPS mass, and aerodynamic trim requirements. Also, volume and dimensional constraints imposed by both the Shuttle payload bay and potential payloads impacted the design. The configuration chosen is illustrated in figure 4. Using an ablative thermal-protection system on a one-pass mission yielded the lightest vehicle and thus the largest payload. The results of a cost analysis also were favorable to the ablator (reference 17).

The payload capability of AMOOS is shown in figure 5, compared to the propulsive OOS. The advantage over a purely propulsive OOS lies in missions to high orbits where the propellant savings as a result of aerobraking

are largest. Another important result of the feasibility studies is that AMOOS is indeed less sensitive than the OOS, to variations in specific impulse and structural mass. This is due to the smaller ΔV requirement which allows for a higher inert mass.

The principal disadvantages to AMOOS lie in the area of navigation and guidance. The combination of navigation errors and uncertainties in the properties of the atmosphere could cause the vehicle either to reenter or fail to dissipate enough energy to effect Shuttle rendezvous. Furthermore, the time histories of most of the trajectory state parameters are indistinguishable for a wide range of atmospheric density variations until the vehicle has very nearly reached its lowest point. This leaves little time to detect errors and make the necessary corrections (reference 18).

Studies (references 16 and 17) have shown that the payload retrieval mission, since it results in the heaviest vehicle at atmospheric entry, has the greatest impact on the design of vehicle systems required for atmospheric flight. Therefore, it will serve as the design mission for this paper. The mission is a return from geosynchronous orbit at 0° inclination to a low altitude phasing orbit at 28.5° inclination. Most of the plane change is done propulsively during the first burn and the remainder is done using the AMOOS lift capability during the single pass through the atmosphere. The mass of the vehicle at entry is 10338 kg and its aerodynamic coefficients are shown in Figure 6.

AMOOS GUIDANCE CONCEPTS

This section is a summary of the potential guidance techniques for AMOOS, some of which depend on the type of mission. However, the basic concept is the same for all. That is, to correct for atmospheric uncertainties the drag of the vehicle is modulated by either raising or lowering the vehicle's planned altitude profile. This can be done either with the main propulsion system or by controlling the vehicle aerodynamically. This study only considered the latter. A study of guidance concepts is contained in the AMOOS literature (reference 18) and some of the material in this document is repeated here.

For the case when the original high energy orbit of AMOOS is in the same plane as that of the Shuttle, no plane change is required of the vehicle during either the orbital coast or the atmospheric portion of the return trajectory. In fact, while in the atmosphere, AMOOS must experience no net lateral force to avoid a costly propulsive plane change maneuver after exiting the atmosphere.

The most obvious way of controlling altitude when there is no lateral force requirement is direct modification of the lift vector via angle-of-attack. This technique can best be used if AMOOS flies inverted, that is, with a bank angle of 180°, to increase control authority. For instance, if the atmospheric density is lower than expected, AMOOS would increase the angle-of-attack to lower the altitude profile, thereby encountering higher density. At the same time, the higher angle-of-attack results in a higher drag coefficient, contributing to a higher rate of deceleration.

If the vehicle were at 0° bank angle, these effects would tend to cancel each other. Thus, using the inverted mode would decrease the amount of angle-of-attack through which the vehicle must rotate to correct its path. A problem with the angle-of-attack control is that the moment of inertia of the vehicle in the longitudinal plane is quite high, making vehicle rotation in that plane difficult.

The inertia is much less about the centerline, which leads to a consideration of bank angle as the means of control. In this mode, the angle-of-attack remains constant and the vehicle would nominally fly at either 90° or 270° bank angle. Off nominal conditions could be corrected by appropriately modulating bank angle up or down depending on the nature of the conditions. The problem with this mode is that it would result in an orbit plane change. This could be eliminated by reversing the bank angle. For instance, the vehicle would nominally be at a bank angle of 90° from the point of entry to perigee and 270° from perigee to exit. However, the vehicle would have to switch quickly, a difficult maneuver, to avoid excessive perturbation of the trajectory. Bank angle modulation was used in the development of a guidance law in reference 18.

AMOOS could benefit from the advantages of the above modes by using some combination of both. It could be that the trajectory could be divided into various segments during which one mode may be more applicable than the other. However, any scheme which would have the advantages of both modes would also have the disadvantages and in addition would be more complex.

Another method discussed in the AMOOS literature is a constant rotation of the vehicle about the velocity vector during the nominal trajectory. This results in no net lateral force. In this case, off-nominal conditions are compensated for by varying the angular rate during appropriate portions of the cycle in such a manner that the average rate remains unchanged over one revolution. The result is a net lift in a direction which may be controlled. The problems of this mode are that it is sensitive to the initial value of bank angle and it requires an almost constant firing of the vehicle's reaction control thrusters.

Most of the missions to high energy orbits require a change in orbit inclination of 28.5°. On the return trajectory a significant portion of this change can be provided aerodynamically (reference 17), with a corresponding decrease in fuel requirements. Controlling AMOOS during the atmospheric pass of such a mission requires bank angle modulation. For instance, the vehicle could fly at the angle of attack for maximum lift and a bank angle of 90°. This would give the greatest plane change capability and the largest possible lift vector available to use as a control. The bank angle could be modulated up or down to correct for uncertainties. This would result in a reduced plane change capability which could be accounted for in the targeting of the nominal trajectory. Since the mission in this study includes a 28.5° plane change, this mode was selected for more detailed study. Moreover, this paper will develop a guidance law which will give only the control history required rather than how the vehicle will achieve a particular bank angle.

SENSITIVITY OF AMOOS TO THE ATMOSPHERE

The sensitivity of AMOOS to variations in atmospheric properties was determined by establishing a nominal trajectory using a mean atmosphere, generating other trajectories using deviations from the mean atmosphere, and comparing the results, all other parameters being equal. Two approaches were taken to generate the various atmospheres; constant multipliers on density and statistical variations of density-altitude profiles.

All of the AMOOS trajectories were calculated with POST, the Program to Optimize Simulated Trajectories (ref. 19). This is a general performance analysis program which has modularized vehicle and planet models and a generalized targeting and optimization capability. It has been used extensively on a variety of problems and includes recent developments in numerical integration and optimization techniques.

The nominal trajectory was calculated using the nominal density profile shown in Table 1, the angle of attack corresponding to maximum lift, and a bank angle of 90° to maximize plane change capability. The trajectory program, POST, was used to calculate the magnitude and angle of the retro burn at geosynchronous altitude which resulted in the desired orbit apogee altitude and inclination upon exit from the atmosphere. An iterative minimum norm technique was used for targeting. In this case, where the number of control variables equals the number of constraints, this reduces to the classical Newton-Raphson technique for finding the

minimum of a function. Trajectory sensitivities were numerically determined using forward differences based on perturbing the control variables.

To achieve an acceptable phasing orbit, AMOOS must exit with an apogee between 500 km and 720 km (reference 17) and an inclination of 28.5°. The nominal was targeted to an apogee of 600 km and an inclination of 28.7° so that when a guidance law is eventually implemented, any remaining slight dispersions from the nominal could be tolerated. In particular, any deviations from the nominal bank angle will result in a lower value for inclination. The values of the trajectory state variables at the point of atmosphere entry, 120 km altitude, were used as initial conditions for all subsequent trajectories.

A series of trajectories was run using different ratios of density encountered to mean density. This ratio remained constant throughout each particular trajectory. The result was a very wide range of apogee altitudes, as shown in figure 7. This figure indicates that very slight variations in density (< 1%) will result in final apogees outside the acceptable range. Density ratios greater than 1.04 result in reentry. For densities only slightly lower than the mean, AMOOS exits the atmosphere with too much velocity to achieve an acceptable phasing orbit. Figure 8 shows the variation of the other critical end condition, orbit inclination, with density ratio. As in the case of final apogee, the range of values here is also very wide. Thus, the amount of velocity addition, and its corresponding fuel penalty, required to correct for errors in inclination is very high. This is shown in figure 9 as a plot of velocity addition required to bring the inclination back to the

desired value of 28.5° versus the amount of inclination correction required at various orbit altitudes.

Constant density ratios throughout a range of altitudes would never occur in nature. Therefore, a more realistic atmosphere variation was simulated using a statistical model of the atmosphere, developed in unpublished NASA research, which models over 6,000 Meteorological Rocket Network soundings of the atmosphere. The model is in the form of a computer program which uses a random number generator, assuming temperature and density are normally distributed, to generate temperature, density, and pressure profiles whose statistical properties and vertical gradients match those of the data. The program also provides the mean, standard deviation and interlayer correlations of the data. This study used atmospheres generated for the spring season in a latitude band of 15° on each side of the equator. Atmospheric data tables were automatically input to POST from the atmosphere generator program.

Of the 300 trajectories calculated, each with a different atmosphere, 137 did not achieve the exit altitude. The final apogees of the remaining trajectories are presented as a histogram in figure 10. This reinforces the conclusion of the previous figure, that AMOOS is extremely sensitive to uncertainties in the properties of the atmosphere.

Further analysis of the state parameters of the trajectories revealed relationships that proved useful in developing a linear feedback guidance law. Figure 11(a) shows the dependence of the final apogee on the vehicle's orbital energy at exit. Since the vehicle is in an elliptic orbit, the values of energy are negative. The curve is smooth

throughout the entire range of trajectories. Figure 11(b) is a magnification of the same data in the region of the desired apogee. The allowable apogee range and the corresponding energy range are indicated. The energy at exit may vary within a band of 500,000 m^2/s^2 and still result in an acceptable trajectory.

Now, the relationship between final energy and energy during the atmospheric pass must be determined. Figure 12 shows the value of energy at the point of perigee versus final energy in the region of interest. The band of allowable values corresponding to the final energy band determined in the preceding figure is shown. The 200,000 m^2/s^2 width of the band can be considered accurate due to the smoothness of the data.

Similar results are shown for orbit inclination in figure 13. This plot of final inclination versus final energy is also smooth and, along with the results of the previous two figures, gives confidence that energy management during an AMOOS pass through the atmosphere would lead to accurate targeting of the trajectory.

GUIDANCE LAW DEVELOPMENT

Based on the previous AMOOS guidance discussion, a linear feedback law for bank angle modulation was chosen for further study. Two approaches were taken to develop this law. First, a relatively simple heuristic law was used to demonstrate the concept. Then an analytical development followed using optimal control theory.

The Heuristic Approach. The first approach was to have the energy of the vehicle follow the energy profile of the nominal trajectory using bank angle as the control. The feedback equation was simply,

$$\phi = \phi_{nom} + K (E_{act} - E_{nom}) \qquad (1)$$

The nominal bank angle, ϕ_{nom}, was a constant 90° and the gain, K, was a constant chosen by trial and error with no attempt at optimization. The desired value of energy, E_{nom}, at each point in the trajectory was taken from an input table of values obtained from the nominal trajectory. In addition, to avoid possible large excursions in bank angle and resulting loss in inclination, the bank angle was limited throughout the trajectories to a minimum value of 50 and a maximum value of 130 degrees.

Various schemes for formulating the nominal energy table were tried. The best results were obtained by inputting energy versus flight path angle. All trajectories that exit the atmosphere must have a perigee point (where flight path angle is zero) and it was shown earlier, in figure 12, that matching values of energy at perigee would be advantageous.

Also, the initial flight path angle was identical for all trajectories and the final flight path angles for all the trajectories with an acceptable final apogee were nearly the same. Therefore, matching a nominal energy versus flight path angle profile results in an acceptable trajectory.

The performance of the heuristic guidance law is illustrated in figure 14. For the range of density factors used the values of final apogee generally fell within the acceptable tolerance. The variation of final orbit inclination is shown in figure 15. The result here is excellent with the inclination never being more than 0.2 degrees from the desired value of 28.5°. Using the results of the last two figures, the level of performance of the heuristic linear feedback guidance law successfully demonstrated the feedback technique and was judged sufficiently high to proceed with an analytical development using optimal control theory.

The Analytical Approach. Since the equations of motion for the atmospheric portion of AMOOS' flight are highly nonlinear, as is typical with entry or skip types of trajectories, the development of an "exact" explicit feedback guidance scheme is not feasible. Therefore a perturbation guidance scheme was developed involving trajectories in the immediate neighborhood of the nominal path. By the proper choice of quadratic performance criteria and quadratic constraints, a feedback law will be synthesized to keep the system within an acceptable deviation from the nominal using acceptable amounts of control.

Following the analysis of Bryson and Ho (ref. 20), the development of the optimal regulator is that of the terminal controller with infinite

final time. The equations of motion of a general system are,

$$\dot{\bar{X}} = \bar{F}(\bar{X}, \bar{U}), \tag{2}$$

where $\bar{X}$ is the n-component state vector and $\bar{U}$ is the m-component control vector. The result of a linear perturbation about a nominal is,

$$\delta\dot{\bar{X}} = \frac{\partial \bar{F}}{\partial \bar{X}} \delta\bar{X} + \frac{\partial \bar{F}}{\partial \bar{U}} \delta\bar{U} \tag{3}$$

For a simpler notation,

$$\text{let } x = \delta\bar{X},\ u = \delta\bar{U},\ A = \frac{\partial \bar{F}}{\partial \bar{X}}\ ,\ \text{and } B = \frac{\partial \bar{F}}{\partial \bar{U}}\ , \tag{4}$$

where A is an n x n and B an n x m sensitivity matrix,

then (3) becomes,

$$\dot{\bar{x}} = A\bar{x} + B\bar{u}\ , \tag{5}$$

a linear system. To achieve an acceptable level of the perturbed state, $\bar{x}$, with a minimum of control correction, $\bar{u}$, the scalar performance index,

$$J = 1/2\ (\bar{x}^T S_f \bar{x})_{t=t_f} + 1/2 \int_{t_o}^{t_f} (\bar{x}^T Q \bar{x} + \bar{u}^T R \bar{u})\ dt, \tag{6}$$

is maintained, where S_f, Q, and R are positive definite matrices (ref.20). In particular, S_f, Q and R are diagonal and,

S_f^{-1} = maximum acceptable value of diag $\bar{x}\ (t_f)\ \bar{x}^T(t_f)$,

Q^{-1} = maximum acceptable value of diag $\overline{xx^T}$,

R^{-1} = maximum acceptable value of diag $\overline{uu^T}$.

The scalar Hamiltonian takes the form

$$H = \bar{\lambda}^T A\bar{x} + \bar{\lambda}^T B\bar{u} + 1/2\ \bar{x}^T Q\bar{x} + 1/2\bar{u}^T R\bar{u} \tag{7}$$

The control, $\bar{u}$, that minimizes (6) is obtained by solving (5) simultaneously with the Euler-Lagrange equations,

$$\dot{\bar{\lambda}} = -\frac{\partial H}{\partial x}, \quad \bar{\lambda}(t_f) = S_f \bar{x}(t_f), \tag{8}$$

$$\frac{\partial H}{\partial u} = 0. \tag{9}$$

Performing the differentiations gives,

$$\dot{\bar{\lambda}} = -A^T\bar{\lambda} - Q\bar{x} \tag{10}$$

and $$B^T\bar{\lambda} + R\bar{u} = 0 \Rightarrow \bar{u} = -R^{-1}B^T\bar{\lambda}. \tag{11}$$

Substituting (11) into (5) and repeating (10) gives the linear two-point boundary-value problem,

$$\dot{\bar{x}} = A\bar{x} - BR^{-1}B^T\bar{\lambda} \qquad \bar{x}(t_o) \text{ given} \tag{12}$$

$$\dot{\bar{\lambda}} = -Q\bar{x} - A^T\bar{\lambda} \qquad \bar{\lambda}(t_f) = S_f\bar{x}(t_f) \tag{13}$$

In the discussion of the solution of the problem, Bryson and Ho show that, for a continuous feedback law,

$$\bar{\lambda} = S\bar{x} \tag{14}$$

Substituting (14) into (12) and (13) gives

$$\dot{\bar{x}} = A\bar{x} - BR^{-1}B^TS\bar{x} \tag{15}$$

and $$(\dot{S}\bar{x}) = -Q\bar{x} - A^TS\bar{x}. \tag{16}$$

Performing the differentiation in (16);

$$\dot{S}\bar{x} + S\dot{\bar{x}} = -A^T S\bar{x} - Q\bar{x} . \tag{17}$$

Substituting (15) into (17) yields

$$\dot{S}\bar{x} + SA\bar{x} - SB\,R^{-1}B^T S\bar{x} = -A^T S\bar{x} - Q\bar{x}, \tag{18}$$

and

$$(\dot{S} + SA - SBR^{-1}B^T S + A^T S + Q)\,\bar{x} = 0. \tag{19}$$

Since, in general $\bar{x} \neq 0$,

$$\dot{S} + SA - SBR^{-1}B^T S + A^T S + Q = 0. \tag{20}$$

Solving for $\dot{S}$ gives,

$$\dot{S} = -SA - A^T S + SBR^{-1}B^T S - Q, \tag{21}$$

which is the matrix Ricatti Equation.

Once S is determined, it can be substituted into (14), which in turn is substituted into (11) giving

$$\bar{u} = -R^{-1}B^T S\bar{x} \tag{22}$$

Now, let $C = R^{-1}B^T S$ and substitute into (23) yielding

$$\bar{u} = -C\bar{x} , \tag{23}$$

the desired linear feedback law.

A regulator is a feedback controller designed to keep a stationary system within an acceptable deviation from a nominal condition. For a stationary system, the matrices A and B are constant. Also, let the matrices Q and R be constant and consider the case of $t_f \to \infty$. Then the matrix Ricatti equation has a possible steady-state finite solution.

That is,

$$\dot{S} = 0 = -SA - A^T S + SBR^{-1}B^T S - Q \text{ gives} \tag{24}$$

$$S(\cdot) \to \tilde{S} \text{ at } t_f \to \infty. \tag{25}$$

where $\tilde{S}$ is the solution of (24).

Then the feedback gain matrix is

$$\tilde{C} = R^{-1} B^T \tilde{S}, \tag{26}$$

and

$$u = -\tilde{C}\tilde{x} . \tag{27}$$

Solution of the Matrix Ricatti Equation. If the system defined by (5) is completely controllable and observable, then there is a unique positive definite solution, $\tilde{S}$, to (24). (See reference 22.) There are several techniques for solving the quadratic equation (24). For this study, a theorem is used to reduce it to a sequence of linear equations, whose solutions converge to $\tilde{S}$. This technique was presented by Kleinman in reference 23. Equation (24) is rewritten as

$$SA + A^T S - SBR^{-1}B^T S + Q = 0. \tag{28}$$

The first step in the procedure is to select a matrix C_o such that $A + BC_o^T$ has all its eigenvalues with negative real parts. Then a sequence of matrices $S_0, S_1, S_2, \ldots$, is formed where the S_i are the solutions of the linear algebraic equations

$$S_i A_i + A^T S_i + C_i R C_i^T + Q = 0, \tag{29}$$

where

$$C_{i+1} = -S_i \, BR^{-1} \tag{30}$$

and

$$A_i = A + B^C T_i \tag{31}$$

$S_i = \hat{S}$ (reference 24).

i

The procedure falls into two phases. First the matrix C_o must be found. If A has all its eigenvalues with negative real parts then $C_o = 0$ satisfies the requirement. If not, computation of C_o is required. However, since B is a vector in this study, the calculation is straightforward. In the second phase, equation (20) is solved. Solution procedures for such equations are well known and the calculations are $S_0, S_1, S_2 \ldots$ toward $\hat{S}$ is quadratic (Reference 23).

Application to AMOOS Guidance. In POST, the trajectory program, the state vector, $\bar{X}$, is defined in a rectangular earth-centered inertial reference frame. For convenience, the state vector in this study will be defined in the same manner. The state vector has three position components and three velocity components. Since the method is to change the altitude profile to control energy, the deviations in the position components will not be controlled. The variations of energy seen in the section on the sensitivity to the atmosphere result principally from changes in velocity. Therefore, the three velocity components of X are the only ones of concern to the feedback law. That is, in this application, the state vector used in the analytical development is assumed to contain only the velocity components. Also, as discussed in the section on AMOOS guidance philosophy, the control vector has only one com-

ponent, bank angle. Therefore, the gain matrix, $\tilde{\epsilon}$, reduces to a vector.

In the analytical development of the regulator, the A and B matrices were assumed constant so that a steady state solution for the gain matrix could be found. However, in a typical AMOOS trajectory, the A and B matrices change drastically and rapidly during a pass through the atmosphere. The approach to the problem was then to choose several points on the nominal flight path, evaluate A and B, choose appropriate Q and R matrices, solve the matrix Ricatti equation for S, and then calculate the resulting gain vector. The results at all of the points were then combined to produce a history of the gain vector throughout the trajectory.

Five points along the nominal path were chosen and the rationale for their selection is as follows. First, the point of perigee was chosen since it is that point at which the effects of an unpredictable atmosphere are greatest and the ability of the vehicle to control its path is the highest. Two points were then selected which essentially marked the boundaries of the region in which the vehicle has effective control. One of these points was shortly after atmospheric entry, while dynamic pressure was increasing, at the threshold of significant aerodynamic forces. The other was chosen to occur at a corresponding degree of aerodynamic force, while dynamic pressure was decreasing near the point of exit. The final two points were chosen to be halfway between the two boundary points and the point of perigee. Thus, the entire flight spectrum was included. These five points, the corresponding state variables, and other important trajectory parameters are listed in Table 2.

The A and B matrices at each of the five points were calculated numerically, using forward differencing. As a check, some of the components were re-calculated using central differencing and various perturbation step sizes, with essentially the same results. Each of the velocity components of the state vector and bank angle were perturbed independently and the resulting changes in F in the questions of motion were calculated. The A and B matrices for the nominal trajectory are presented in Table 3.

The Q and R matrices were then calculated as previously described:

Q^{-1} = maximum acceptable value of diag $\overline{xx}^T$

R^{-1} = maximum acceptable value of diag $\overline{uu}^T$.

The process of selecting "acceptable" values of $\overline{xx}^T$ and $\overline{uu}^T$ was a combination of two factors. The first involved analyzing the results of the atmospheric sensitivity study and the heuristic development. The second was to calculate gain vectors using several values for Q and R, testing these with a small number of different atmospheres, and observing their performance.

The maximum allowable deviation in bank angle finally chosen was 30°, the same as that used in the heuristic law. Thus,

$$R = \frac{1}{900} \quad .$$

The Q matrix used was determined by assuming that the maximum deviation allowed in energy was 100,000 m^2/s^2 throughout the trajectory. This was

translated into allowable deviations in the velocity components as follows. The equation for energy per unit mass is the sum of the kinetic and potential energies and is given by,

$$E = 1/2V^2 - \frac{\mu}{r} \quad , \tag{32}$$

where V is the magnitude of the velocity vector, r is the magnitude of the position vector, and μ is the gravitational constant. This form of the energy equation assumes potential energy is zero at infinite radius. As discussed previously, the effect of changes in r is neglected and the change in energy is given by,

$$\frac{\partial E}{\partial V} = V. \tag{33}$$

Then,

$$\Delta E = V\Delta V. \tag{34}$$

But

$$V^2 = (V_1^2 + V_2^2 + V_3^2)^{1/2} \quad , \tag{35}$$

and

$$V\Delta V = V_1\ \Delta V_1 + V_2\ \Delta V_2 + V_3\ \Delta V_3 \quad , \tag{36}$$

where V_1, V_2, and V_3 are the velocity components of the state vector. It was assumed that each component contributed equally to deviations in energy. Therefore, at each point in the trajectory,

$$V_i\ \Delta V_i = \frac{\Delta E}{3} \text{ or} \tag{37}$$

$$\Delta V_i = \frac{10^5}{3V_i} \qquad i = 1, 2, 3 \tag{38}$$

Then,

$$Q_{i_j} = \frac{1}{(\Delta V_i)^2} \quad i = j \qquad i,j = 1, 2, 3$$
$$= 0 \qquad i \neq j \tag{39}$$

The Q matrix for each of the five trajectory points is presented in Table 4.

From reference 20, the system $\dot{x} = Ax + Bu$ is completely controllable if the rank of the composite matrix $(B, AB, A^2 B)$ is 3. The A and B matrices at each of the five points were used to generate the composite matrix and at each point the rank of the matrix was three. Thus, the system is completely controllable. The system is completely observable if there is a matrix D such that

$$DD^T = Q. \quad \text{(Reference 21)} \tag{40}$$

The matrix Q is diagonal and is defined in (39) as,

$$Q_{i_j} = \frac{1}{V_i^2} \quad i = j \qquad i,j = 1,2,3.$$
$$= 0 \qquad i \neq j$$

The matrix D, then, is also diagonal and can be defined as

$$D_{i_j} = Q_{i_j} = \frac{1}{V_i} \quad i = j \qquad i,j = 1,2,3. \tag{41}$$
$$= 0 \qquad i \neq j$$

Therefore a matrix which satisfies (40) exists and the system is completely observable. The controllability and observability requirements are satis-

fied and the matrix Ricatti equation has a unique positive definite solution.

This solution was found and the gain vector at each point was calculated using a NASA developed computer program. All of the A matrices had eigenvalues with negative real parts, thus the first phase of the Ricatti equation solution was omitted. All of the solutions converged rapidly and the resulting gains are presented in figure 16. Since all three curves were smooth, no more trajectory points were required; the values of gain between the points could be determined by interpolation.

The guidance law was synthesized into the trajectory program according to the following block diagram.

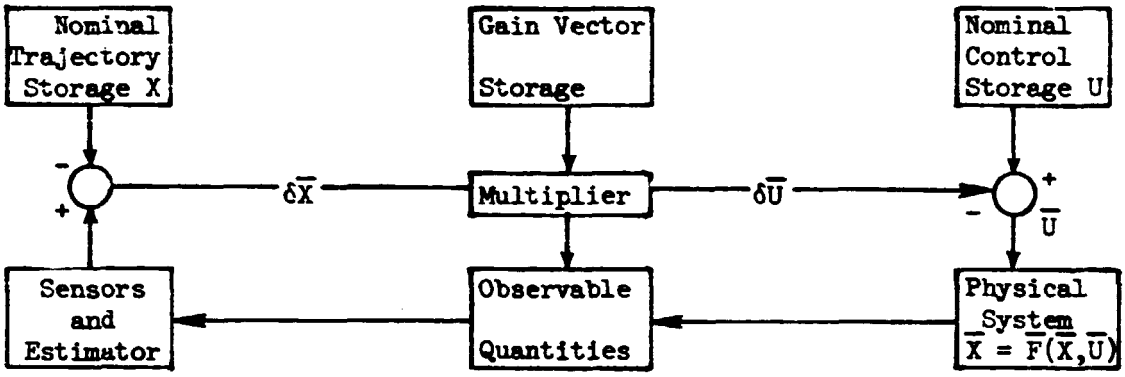

The nominal trajectory and the gain vector were stored versus flight path angle as tables with cubic interpolation, while the nominal control was constant. The bank angle again had fixed limits of 50 and 130 degrees. For this analysis, perfect knowledge of the state was assumed.

The feedback guidance law developed was tested on a number of atmospheres provided as before with the statistical atmosphere generator

program. The performance of the law is illustrated by the histogram in figure 17. Out of the 50 trajectories run, 4 failed to exit from the atmosphere. Nearly all of the final apogees were lower than desired. However, about 72% fell within a 200 Km tolerance, and about 91% were within a 300 Km spread. The mean of the 46 apogee values is 260.6 Km and the standard deviation is 125.6 Km. In addition, all of the values of final inclination for these trajectories were between 27.05° and 27.91°. The bank angle histories of these trajectories tended to switch from one fixed limit to the other, as illustrated in figure 18. The behavior of this particular history is typical. This is most likely due to the difficulty of representing the nominal trajectory in a meaningful manner in the chosen reference frame. The parameters that can describe a trajectory vary widely near the point of perigee throughout the range of atmospheres used and, except for energy, there is no particular reason to constrain any of them. Therefore, representing the desired state vector as a function of one of the parameters may not have completely satisfactory results.

CONCLUSIONS AND RECOMMENDATIONS

The Aeromaneuvering Orbit-to-Orbit Shuttle (AMOOS) concept for a reusable upper stage to be carried by the Space Shuttle has been shown to be highly sensitive to unpredictable variations in the density of the atmosphere through which it flies. This was done using a large number of atmosphere variations whose statistical properties match those of actual data. If the vehicle is not able to compensate for these variations, it may fail either to exit from the atmosphere or to dissipate enough energy to establish an acceptable phasing orbit with the Space Shuttle. Therefore, a guidance law that can compensate for the variations is crucial to the feasibility of the AMOOS concept.

A heuristic linear feedback guidance law was developed which demonstrated that such a law could control the trajectory within acceptable tolerances. This law was designed to hold the energy of the vehicle to the energy profile of the nominal trajectory. It was tested on a number of different atmospheres using constant multipliers to provide density variations.

An optimal regulator was synthesized using modern control theory. The resulting feedback law, based on linearized equations of motion and a study-state assumption, demonstrated the feasibility of this technique. This law was tested using the statistically varying atmospheres and the values of final orbit apogee were generally lower than the desired value but within a 300 Km band. Also, there was a tendency for the bank angle to switch from one fixed limit to the other during a trajectory.

Several refinements can be made to the technique to improve performance and ease the bank angle switching. One is to define the state vector in a more natural reference frame, allowing direct control of important parameters such as total velocity. A likely candidate for such a reference frame is one which defines the position vector by altitude, latitude and longitude and the velocity vector by velocity magnitude, flight path angle, and heading angle. Another advantage of this system is that the sensitivity matrices can be easily determined explicitly rather than numerically. An even more direct approach would be to use energy itself as a state variable (reference 24). This would have the additional benefit of reducing the dimensionality of the system.

The limitations of linearization could also be reduced. Not only is the physical system naturally non-linear but there is a random term introduced by the uncertain variations in the properties of the atmosphere. A continuous random process term could be added to the equations of motion. This term could also be used to account for the absence of higher order terms when the system is linearized. The analysis of such a system is discussed in tutorial fashion in reference 25.

The feasibility of AMOOS depends absolutely on its ability to compensate for unpredictable density variations encountered during the atmospheric portion of the flight. A feedback guidance law which provides this crucial capability has been developed. Possible refinements to the development of the law to further improve its performance have also been proposed.

REFERENCES

1. National Aeronautics and Space Administration, "Baseline Tug Definition Document, Revision A," PD-DO-SI (72-56), Marshall Space Flight Center, Alabama, June 26, 1972.

2. Tug Operations and Payload Support Study, Volume 2, Representative Mission Options and Payloads Selection, North American Rockwell Report, SD 73-SA-0006-2. March 5, 1973.

3. London, H. S.: Change of Satellite Orbit Plane by Aerodynamic Maneuvering. IAS 29th Annual Meeting, New York, N. Y., 1961.

4. Nyland, F. S.: The Synergetic Plane Change for Orbiting Spacecraft. RM-3231-PR, Rand Corp., Santa Monica, Calif., 1962.

5. Bell, R. N., and Hankey, W. L., Jr.: Application of Aerodynamic Lift in Accomplishing Orbital Plane Change. ASD-TDR-63-693, ASD 1963 Science and Engineering Symposium, September 1973.

6. Bruce, Richard W.: The Combined Aerodynamic-Propulsive Orbital Plane Change Maneuver. AIAA Paper 65-20. AIAA 2nd Aerospace Sciences Meeting, New York, N.Y., January 1965.

7. Cuadra, E., and Arthur, Paul D.: Orbit Plane Change by External Burning Aerocruise. AIAA Paper 65-21. AIAA 2nd Aerospace Sciences Meeting, New York, N.Y., January 1965.

8. Paine, J. P.: Some Considerations on the Use of Lifting Reentry Vehicles for Synergetic Maneuvers. AIAA Paper 66-960, Third Annual Meeting, December 1966.

9. Clausss, J. S., Jr. and Yeatman, R. D.: Effect of Heating Restraints on Aeroglide and Aerocruise Synergetic Maneuver Performance. AIAA Paper 67-169, AIAA 5th Aerospace Sciences Meeting, New York, N.Y., January 1967.

10. Maslen, S. H.: Synergetic Turns with Variable Aerodynamics. AIAA Spacecraft, November 1967, pp. 1475-1482.

11. Roessler, M.: Optimal Aerodynamic-Propulsive Maneuvering for the Orbital Plane Change of a Space Vehicle. AIAA Spacecraft, December 1967, pp. 1678-1680.

12. Dickmanns, E. D.: The Effect of Finite Thrust and Heating Constraints on the Synergetic Plane Change Maneuver for a Space Shuttle Orbiter-Class Vehicle. NASA TN D-7211, October 1973.

13. Kostoff, R. N.: Aerobraking the Space Tug from Synchronous Orbit into Low Circular Earth Orbit; Guidance and Heating Constraints in First Atmospheric Pass - Case 237. Memo B71-07031, Bellcom, Inc., Washington, D. C., July 15, 1971.

14. Kostoff, R. N.: Analytic Modeling of an Aerobraking Pass - Case 237. Memo B72-01005, Bellcom, Inc., Washington, D. C., January 19, 1972.

15. Corso, C. J., et al: Space Tug Aerobraking Study. Boeing Document No. D5-17142, The Boeing Co., Huntsville, Ala., April 12, 1972.

16. Andrews, C. D.: Feasibility and Tradeoff Study of an Aeromaneuvering Orbit-to-Orbit Shuttle (AMOOS). LMSC-HREC TR-D306600, Lockheed Missiles and Space Company, Huntsville, Ala., June 1973.

17. White, J.: Feasibility and Tradeoff Study of an Aeromaneuvering Orbit-to-Orbit Shuttle (AMOOS), Final Report. LMSC-HREC TR-D390272, Lockheed Missiles and Space Company, Huntsville, Ala., July 1974.

18. White, J. and Wernli, A.: Guidance Concepts for the Aeromaneuvering Orbit-to-Orbit Shuttle. LMSC-HREC TM-D306356, Lockheed Missiles and Space Company, Huntsville, Ala., August 1974.

19. Brauer, G. L., et al: Final Report, Program to Optimize Simulated Trajectories. MCR-73-206, Martin Marietta Corp., Denver Co.

20. Bryson, A. E., Jr. and Ho, Yu-Chi: Applied Optimal Control. Waltham, Mass., Ginn and Company, 1969.

21. Anderson, B. D. O. and Moore, J. B.: Linear Optimal Control. Englewood Cliffs, N. J. Prentice-Hall, Inc., 1971.

22. Rublein, G.: Final Report, Task Order NAS1-9461-9. The College of William and Mary for NASA-Langley Research Center.

23. Kleinman, D. R.: On an Iterative Technique for Ricatti Equation Computations. IEEE Transactions on Automatic Control, February 1968, p. 114.

24. Bryson, A. E., Jr. and Desai, M. N.: Energy-State Approximation in Performance Optimization of Supersonic Aircraft. AIAA J. Aircraft, Nov.-Dec., 1969, pp. 481-488.

25. Athans, M.: The Role and Use of the Stochastic Linear-Quadratic-Gaussian Problem in Control System Design. IEEE Transactions on Automatic Control, December 1971, pp. 529-552.

TABLE 1. PROPERTIES OF THE MEAN ATMOSPHERE

Altitude, Km	Temperature, °K	Pressure, N/m^2	Density Kg/m^3
60	260.704	25.03130	3.3448×10^{-4}
63	255.631	16.96214	2.3116
66	241.549	11.17573	1.6118
69	210.874	6.99571	1.1557
72	208.266	4.31924	7.2249×10^{-5}
75	204.926	2.64073	4.4892
78	198.660	1.69238	2.9678
81	193.234	1.01280	1.8259
84	188.414	.59284	1.0961
87	181.442	.35945	6.9015×10^{-6}
90	177.810	.20334	3.9839
93	171.758	.11467	2.3258
96	182.265	.06354	1.2145
99	188.930	.03618	6.6713×10^{-7}
102	201.930	.02179	3.7592
105	216.930	.01358	2.1808
108	231.930	.00874	1.3128
111	251.930	.00581	8.0341×10^{-8}
114	281.930	.00401	4.9550
117	311.930	.00288	3.2164
120	341.930	.00213	2.1701

TABLE 2. TRAJECTORY PARAMETERS AT CERTAIN POINTS IN THE NOMINAL FLIGHT PATH

Time, s	Altitude, Km	Velocity, m/s	Flight Path Angle, Deg.	Energy, 10^6 m^2/s^2	V_1,m/s	V_2,m/s	V_3,m/s
0	120	10313.8	-4.57707	-8.154	-9532.6	- 810.5	-3853.2
50	87.374	10326.1	-2.65267	-8.336	-9483.2	-1281.3	-3880.2
90	73.779	10054.7	-1.16388	-11.232	-9125.8	-1608.8	-3902.4
130	70.076	9259.0	.00553	-18.951	-8193.7	-1814.0	-3911.8
190	74.733	8337.9	.87191	-27.011	-7076.1	-2133.7	-3859.7
250	83.810	8053.0	1.1847	-29.260	-6609.4	-2589.3	-3803.1
431	120	7950.3	1.60555	-29.744	-5802.2	-4098.2	-3570.3

TABLE 3. THE A AND B MATRICES AT CERTAIN POINTS ON THE FLIGHT PATH

TIME, S	$A = \frac{\partial F}{\partial X}$			$B = \frac{\partial F}{\partial U}$
50	-.0003506	-.0000222	-.0001592	.0020488
	-.0000291	-.0001793	-.0000195	-.01437
	.0000909	.0000132	-.0001720	-.0001894
90	-.0029458	-.0002530	-.0013612	.020855
	-.0002750	-.0015348	-.0002318	-.117939
	.0007453	.0001343	-.0014670	.0000731
130	-.0047873	-.0005259	-.0023296	.037871
	-.0004970	-.0025692	-.0005065	-.177564
	.0011226	.0002438	-.0024711	.0029141
190	-.0019410	-.0002941	-.0010043	.018024
	-.0002363	-.0011034	-.0002894	-.065491
	.0004139	.0001145	-.0010606	.003010
250	-.0004407	-.0000872	-.0002313	.0049491
	-.0000622	-.0002668	-.0000835	-.014419
	.0000918	.0000313	-.0002489	.0011728

TABLE 4. THE Q MATRIX AT CERTAIN POINTS ON THE FLIGHT PATH

TIME, s	Q MATRIX		
50	.08094	0	0
	0	.0014776	0
	0	0	.013550
90	.074952	0	0
	0	.0023294	0
	0	0	.013706
130	.06042	0	0
	0	.0029615	0
	0	0	.013772
190	.04506	0	0
	0	.0040974	0
	0	0	.013408
250	.03931	0	0
	0	.006034	0
	0	0	.01302

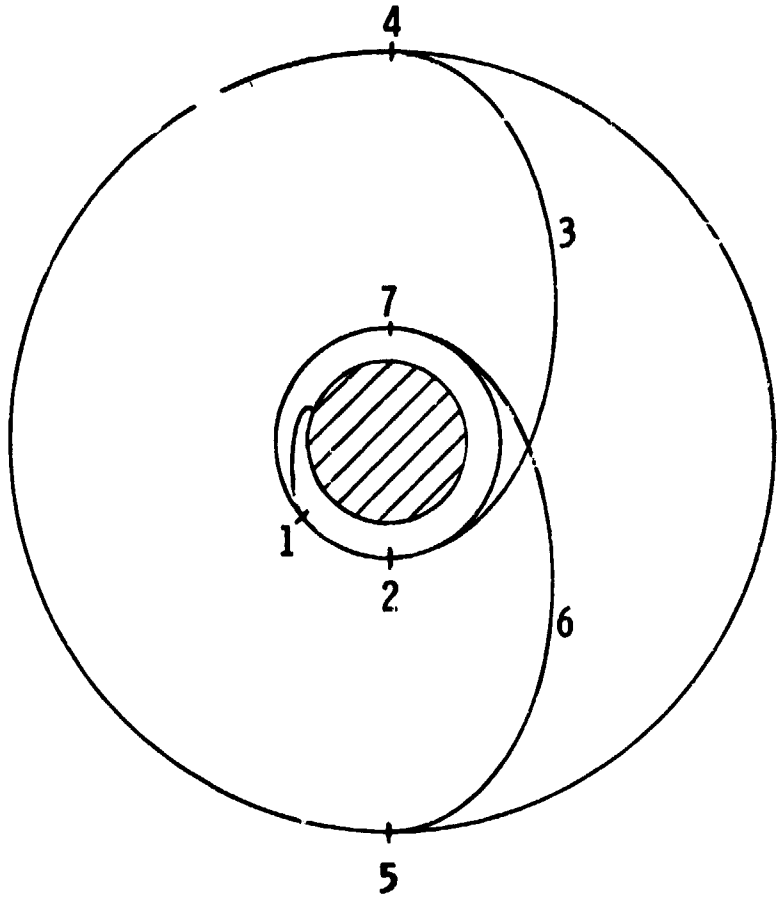

1. Delivered to circular Orbit by Space Shuttle
2. Burn to mission transfer orbit
3. Midcourse correction
4. Burn to mission orbit
5. Burn to return transfer orbit
6. Midcourse correction
7. Burn to Shuttle rendezvous orbit

Figure 1. - Schematic of Propulsive OOS Mission Profile

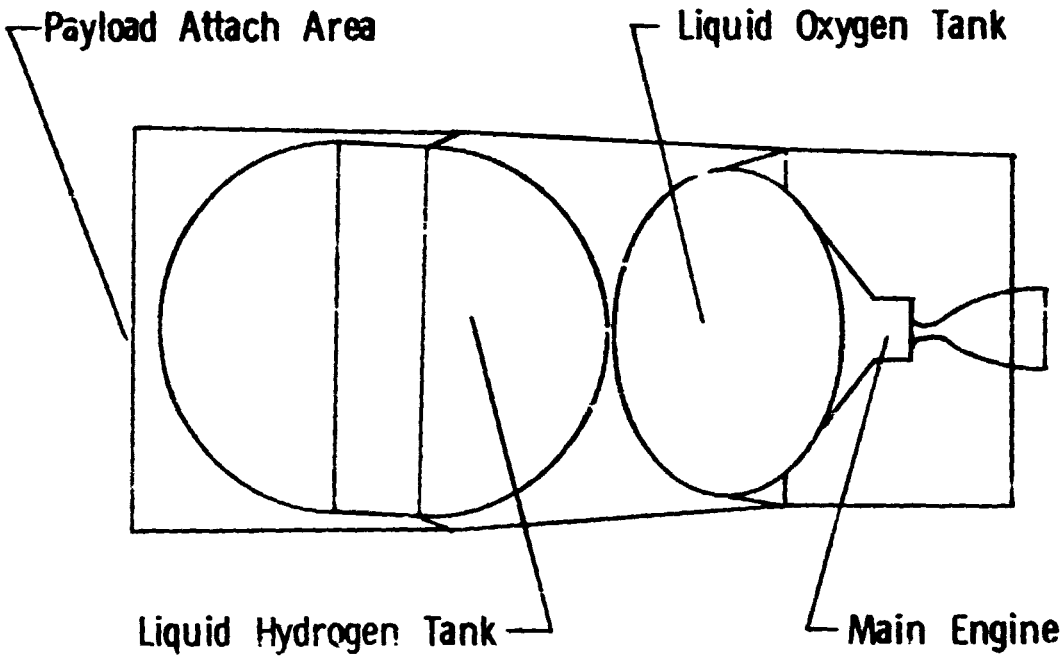

Figure 2. - Schematic of Propulsive OOS Configuration

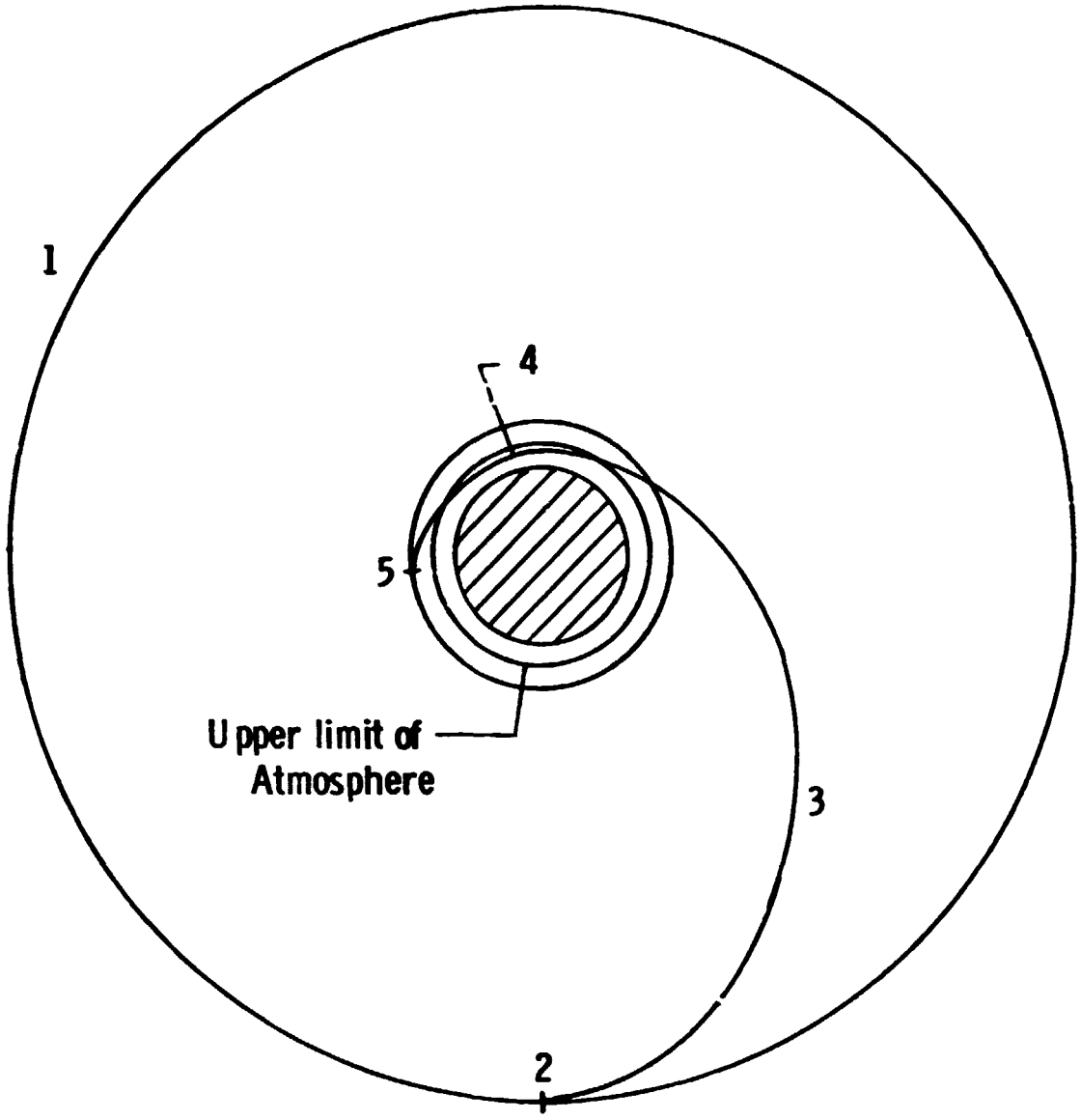

1. Geosynchronous orbit
2. Burn to transfer to aeromaneuvering orbit
3. Midcourse correction
4. Aeromaneuver to phasing orbit plane and apogee
5. Phasing orbit apogee, burn to achieve phasing orbit perigee

Figure 3. - Schematic of AMOOS return trajectory

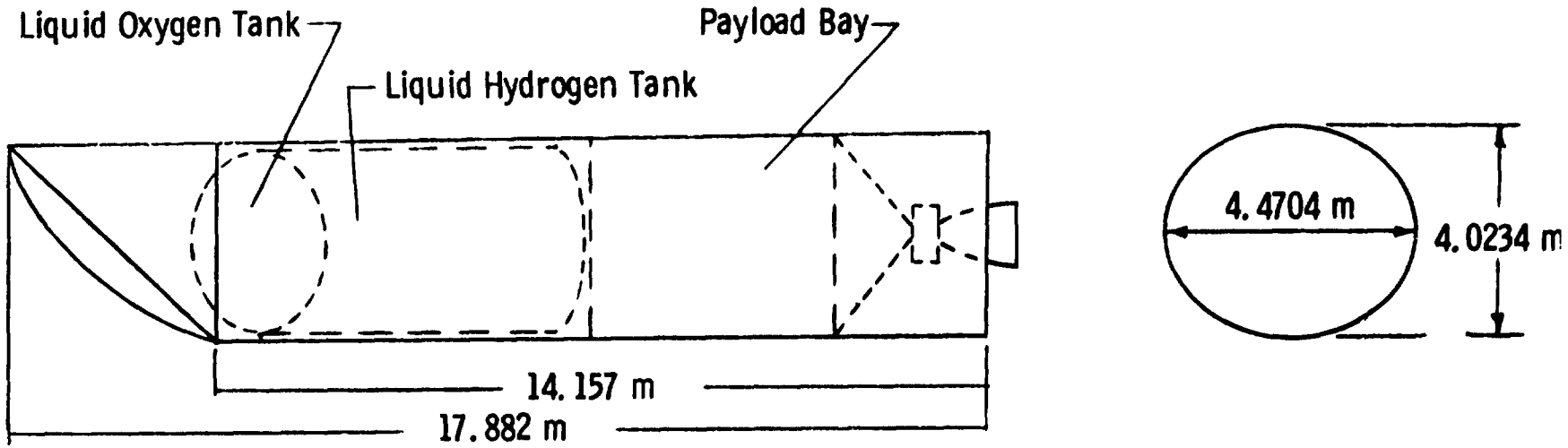

Figure 4. -AMOOS vehicle configuration

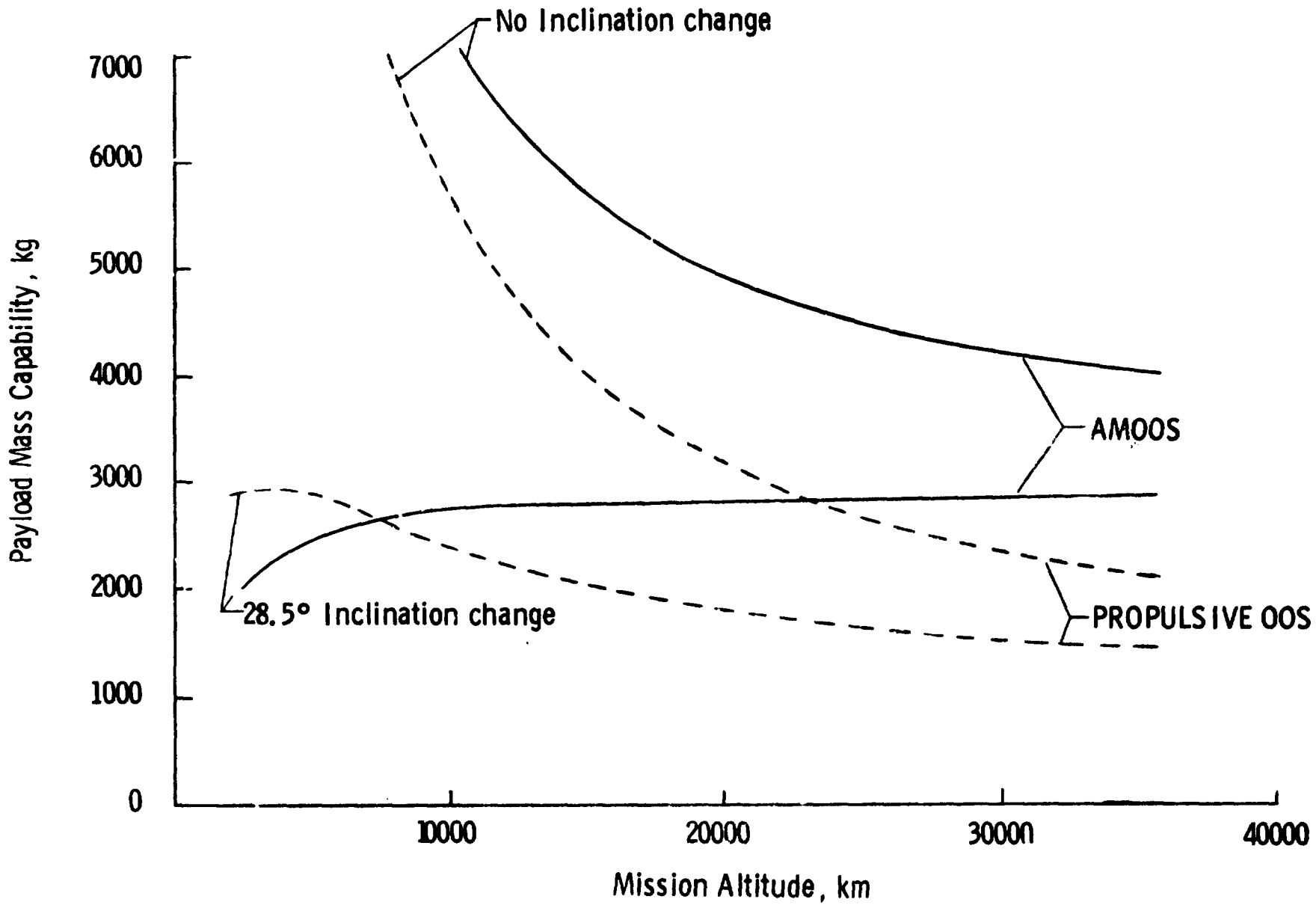

Figure 5. - Comparison of AMOOS and propulsive OOS payload capability

Mach number = 10.27
Reference Area = 15.69 m^2

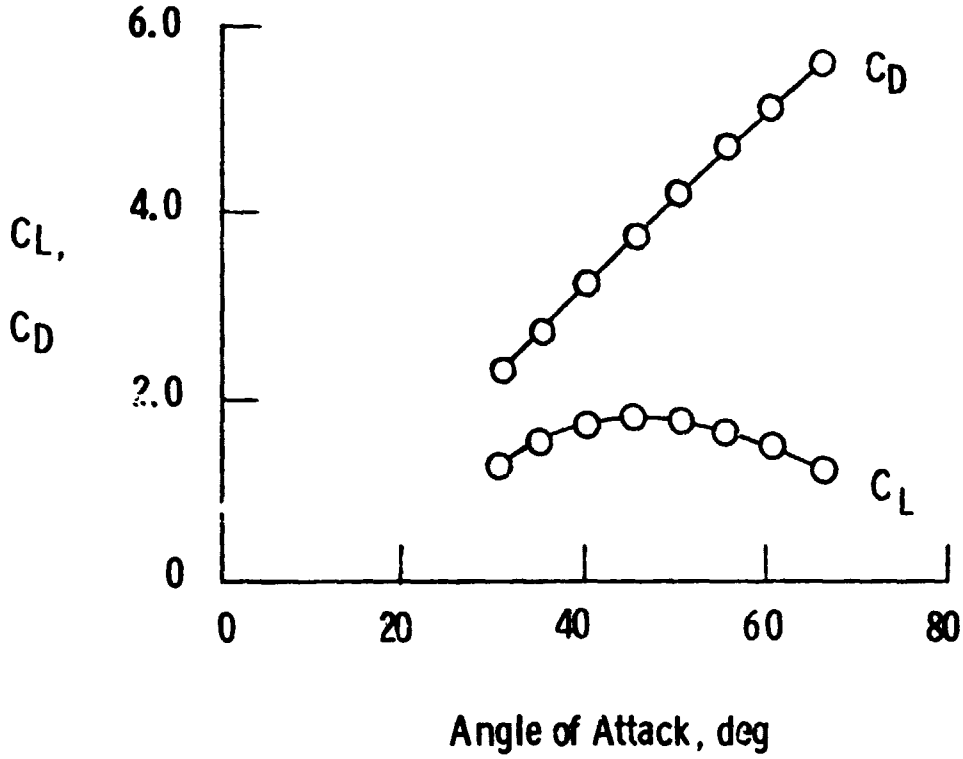

Figure 6. - AMOOS hypersonic lift and drag coefficients

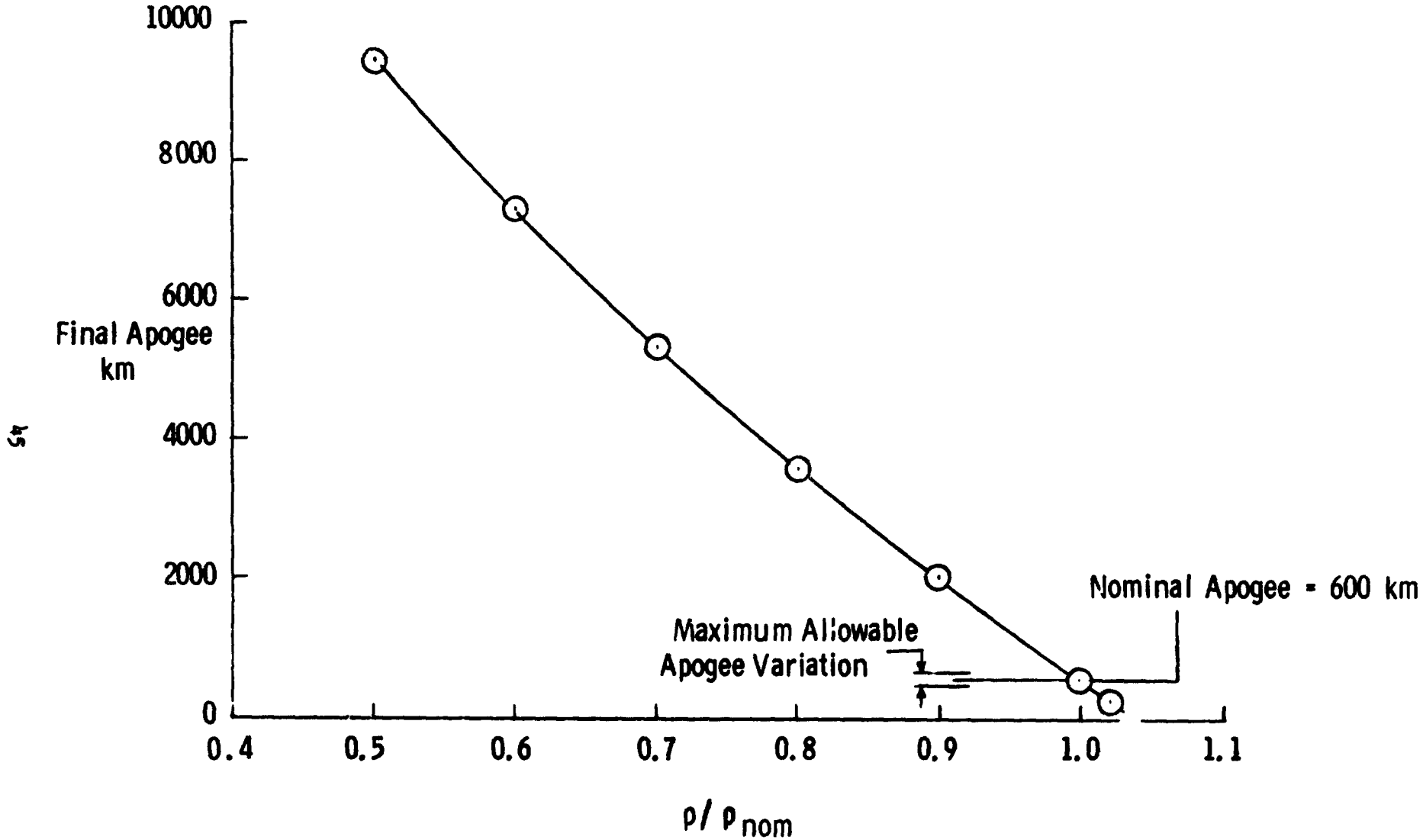

Figure 7. - Variation of final apogee with density factor

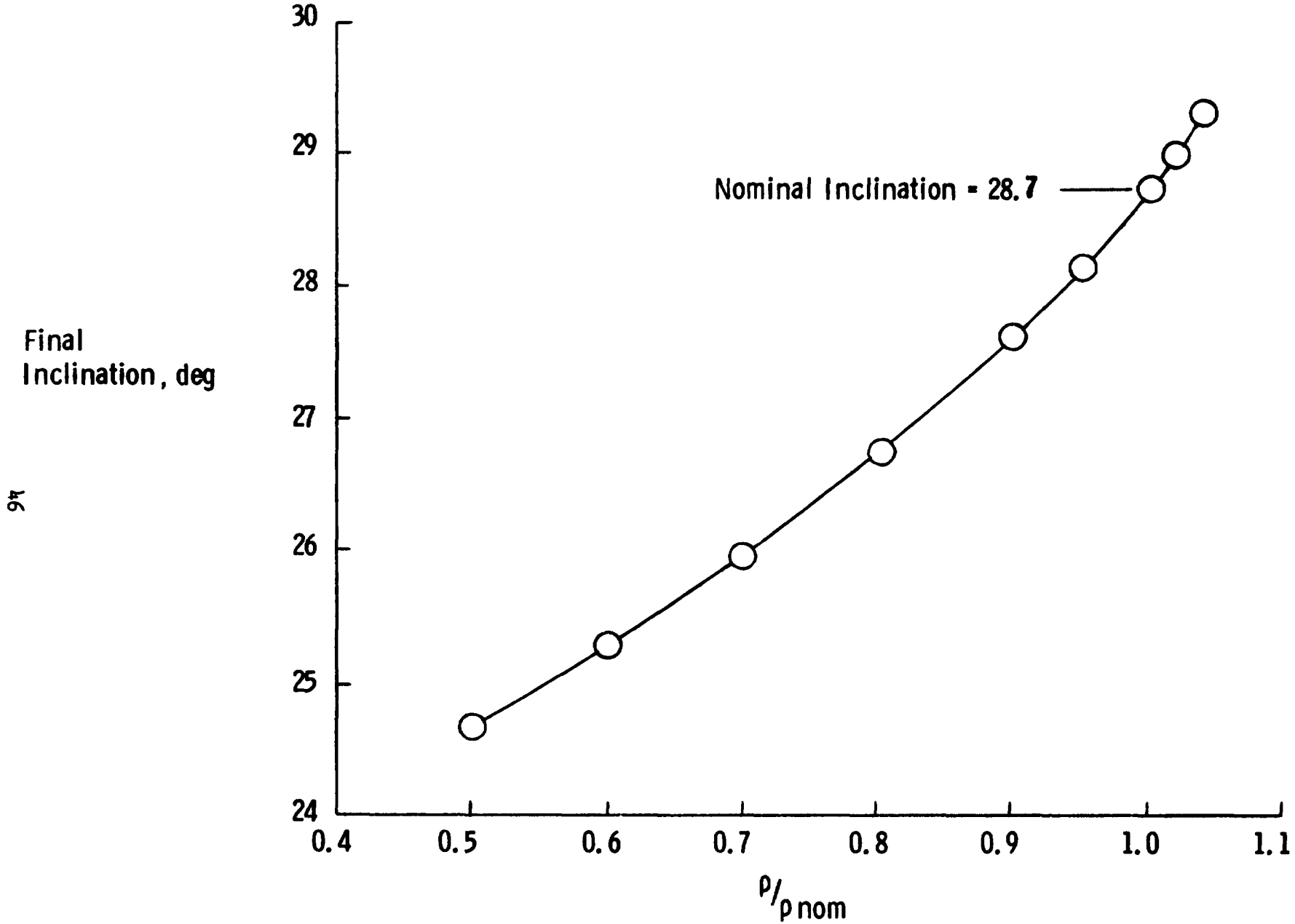

Figure 8. - Variation of final inclination with density factor

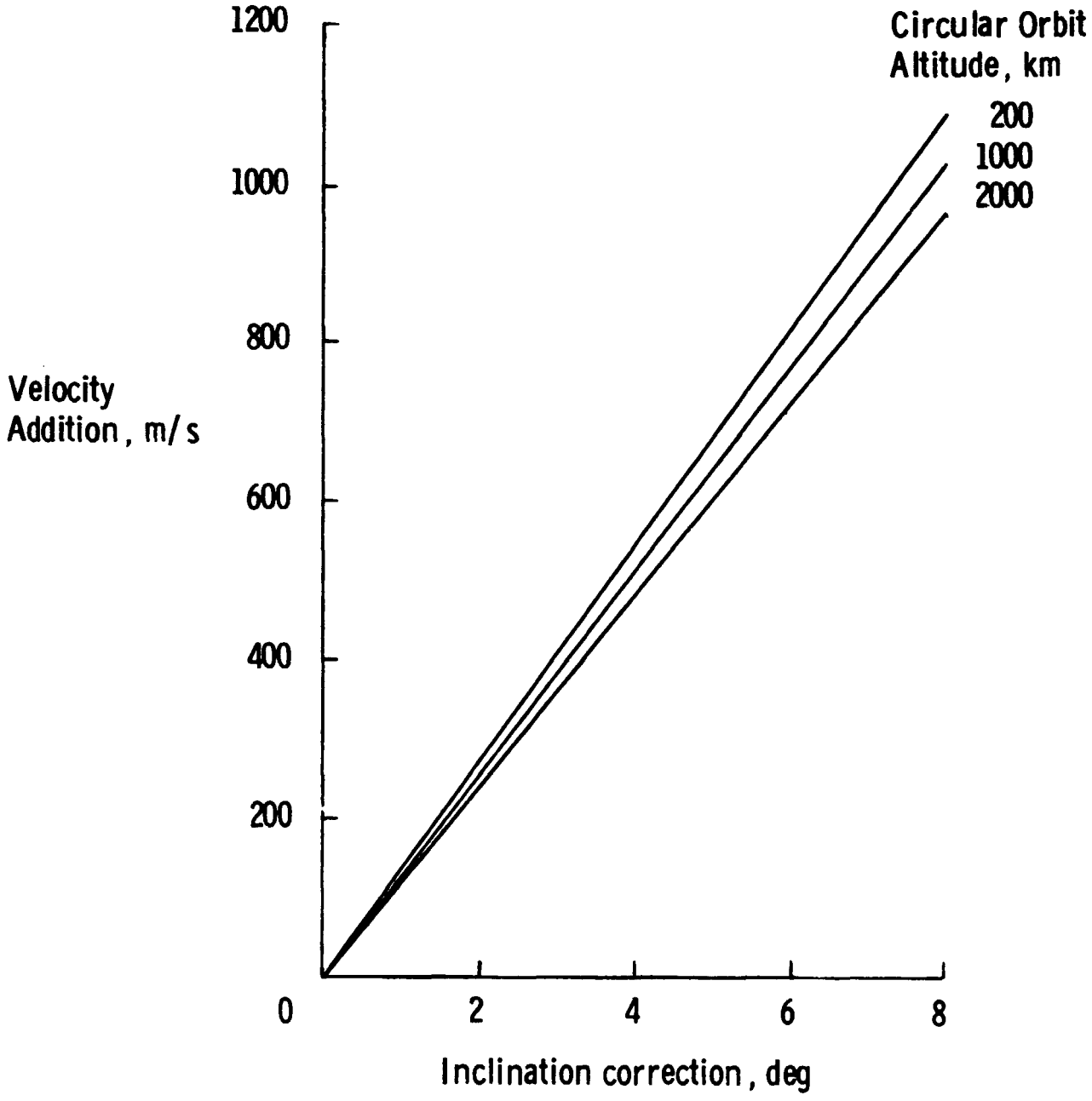

Figure 9. - Velocity addition required to correct inclination error

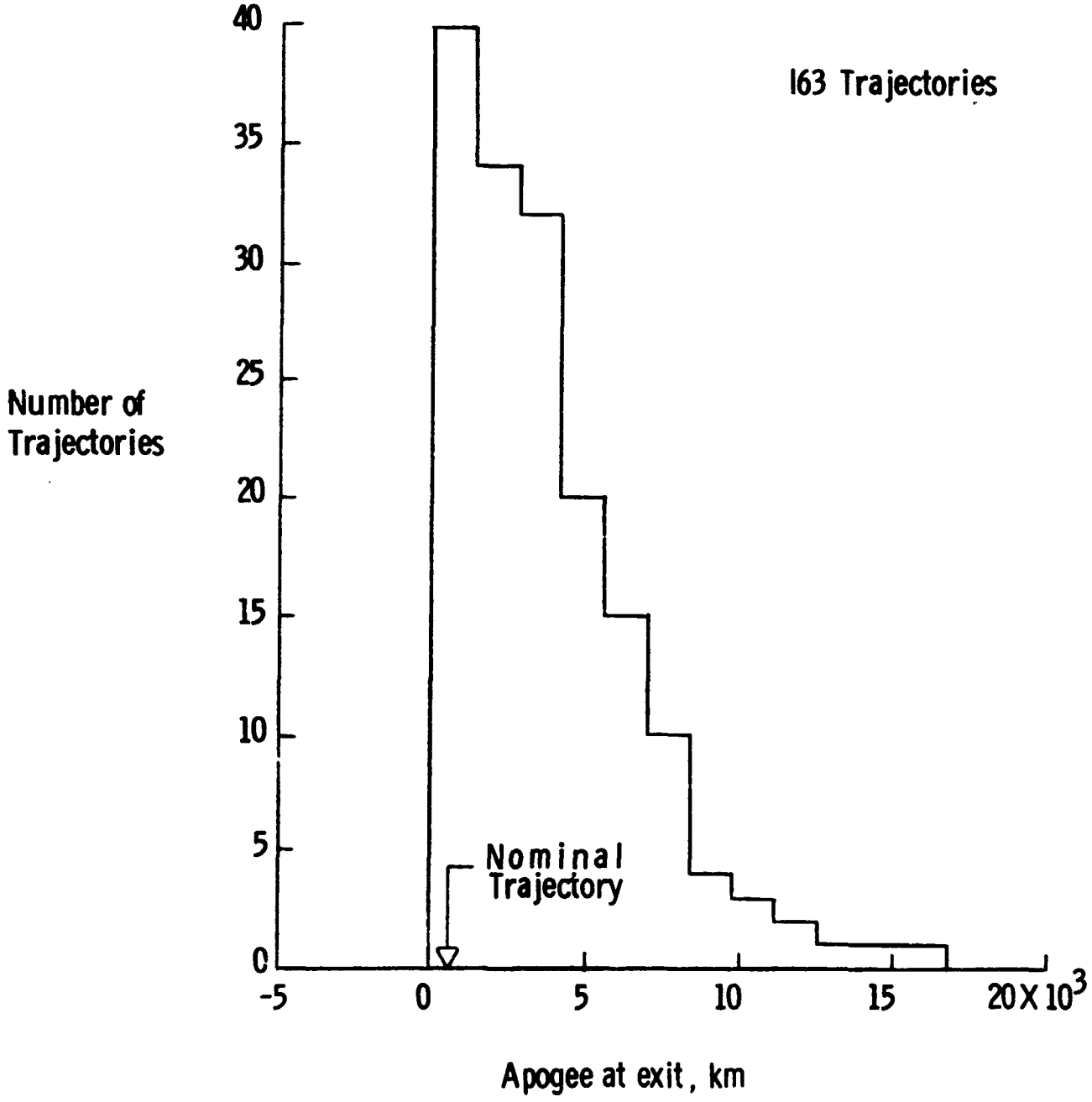

Figure 10. - Histogram of final apogee

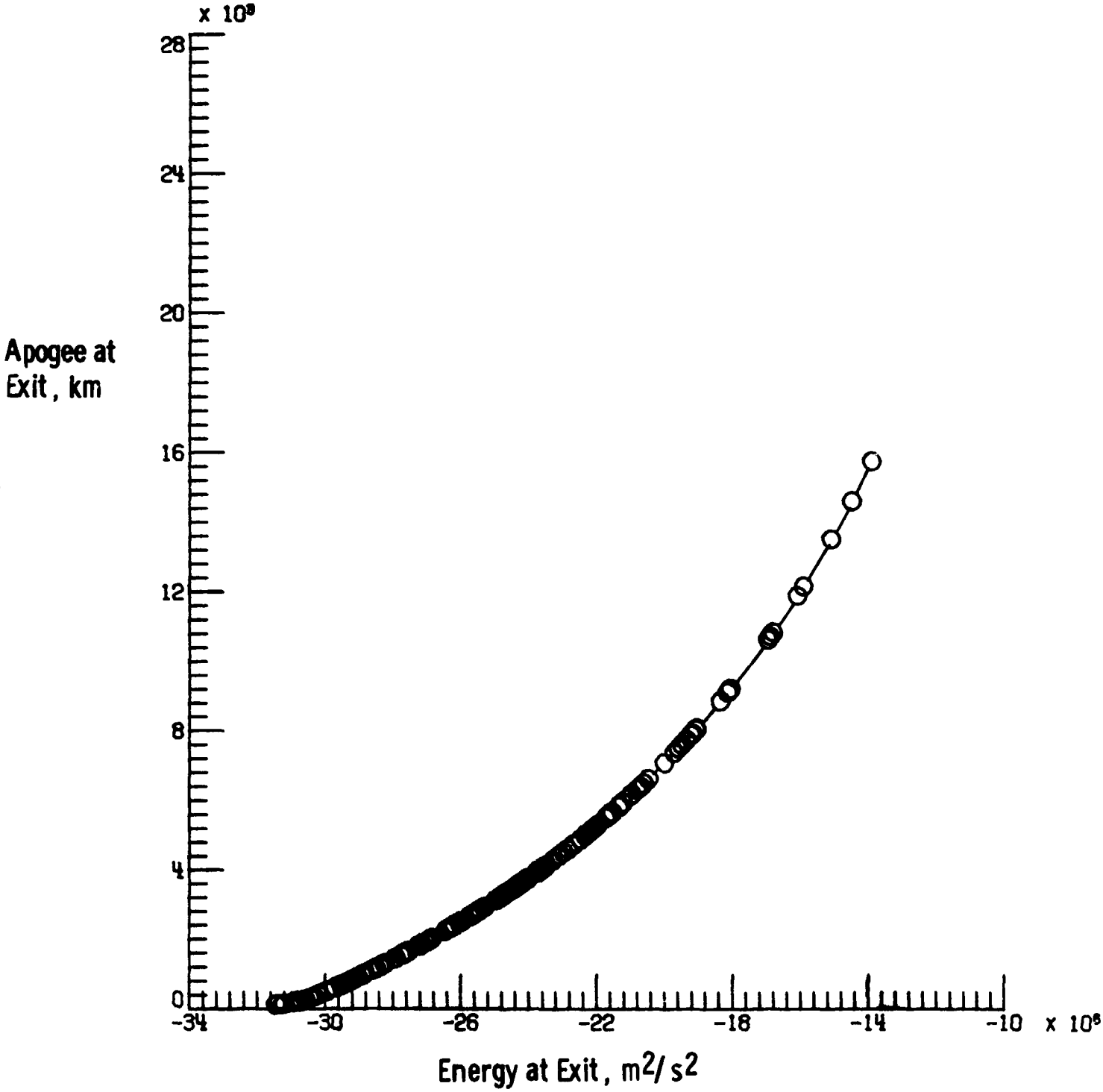

Figure 11 (a). - Variation of final apogee with final energy

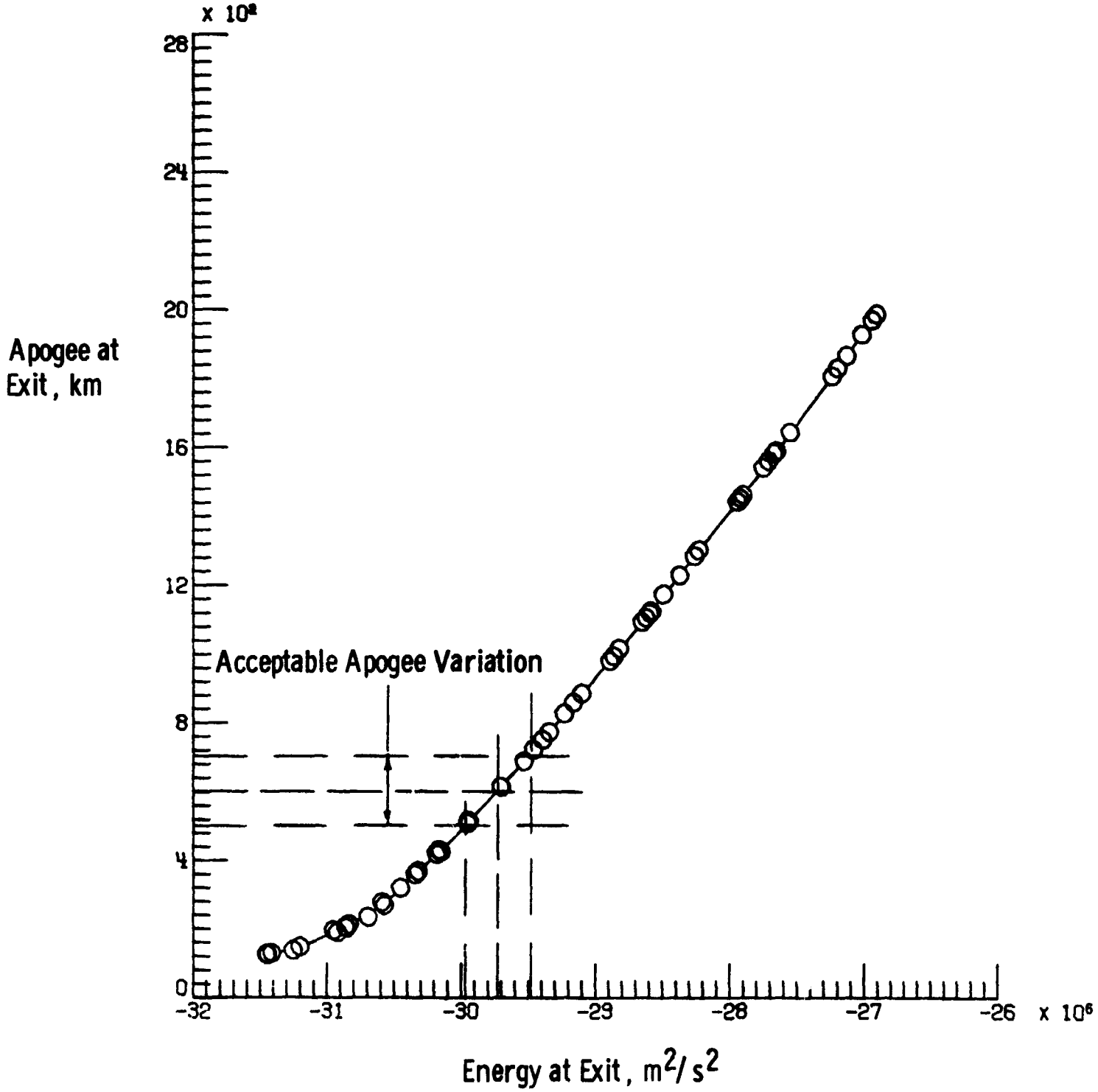

Figure 11 (b). - Magnified view showing acceptable apogee variation

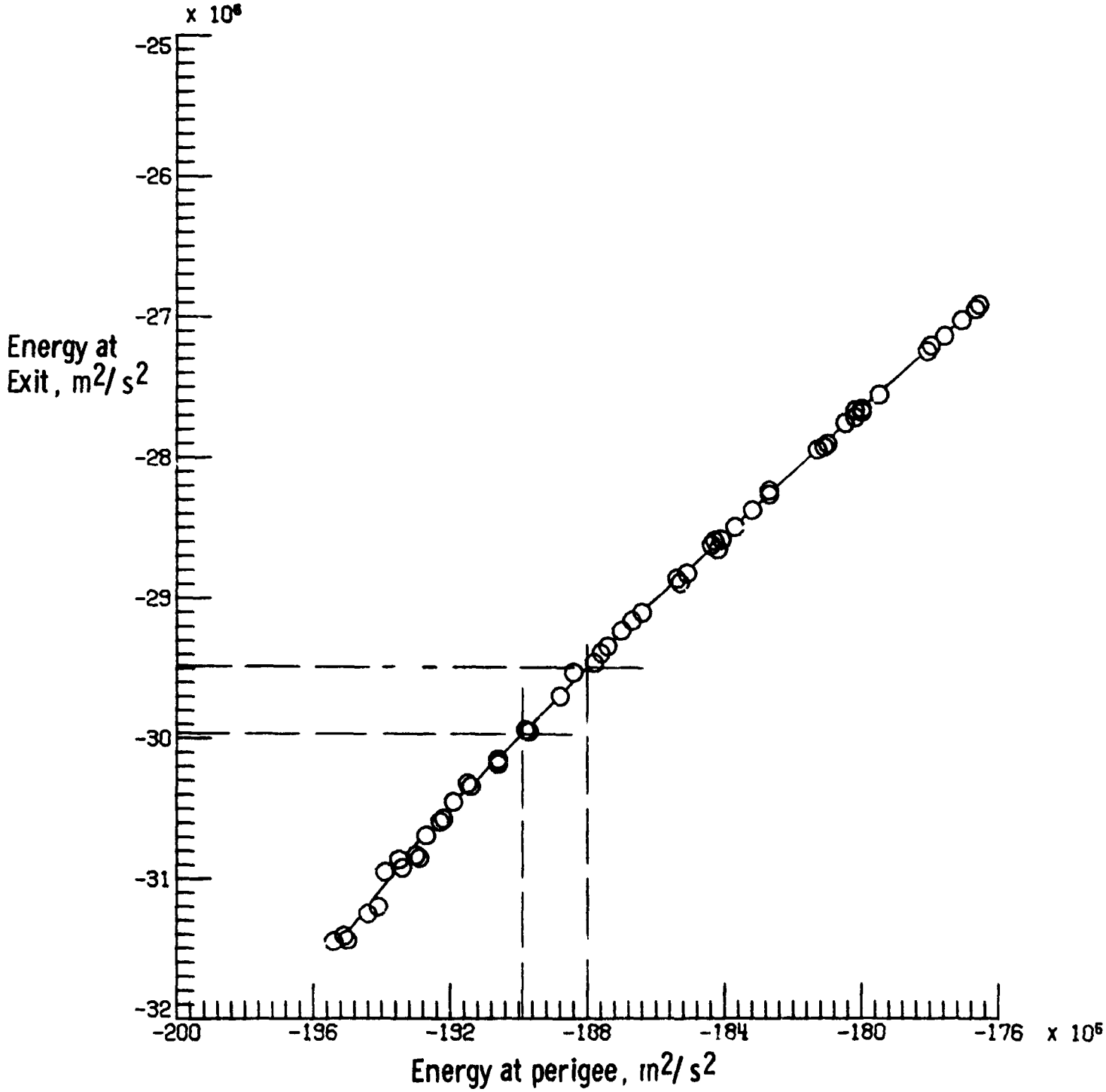

Figure 12. - Variation of final energy with energy at perigee

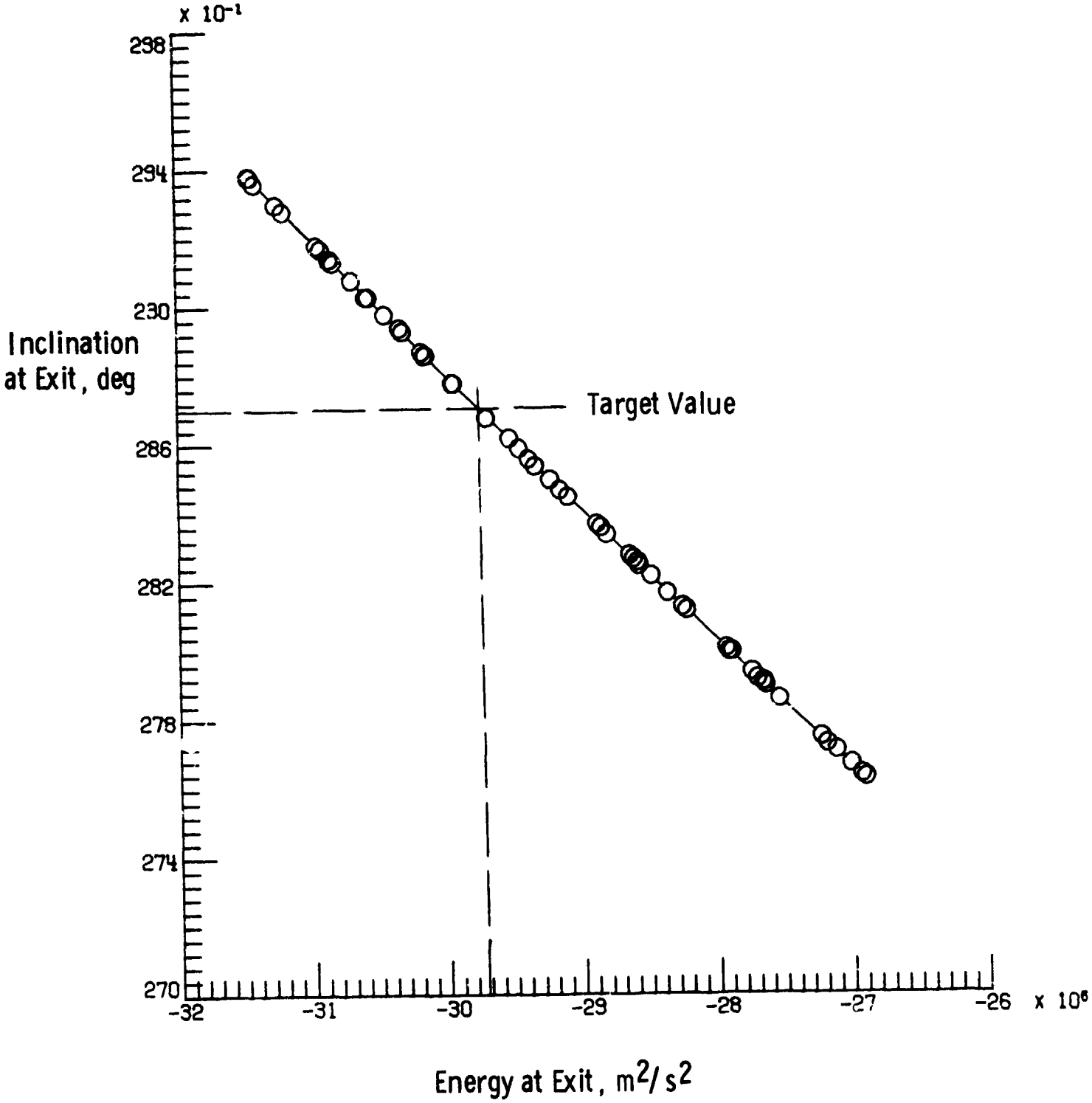

Figure 13. - Variation of final orbit inclination with final energy

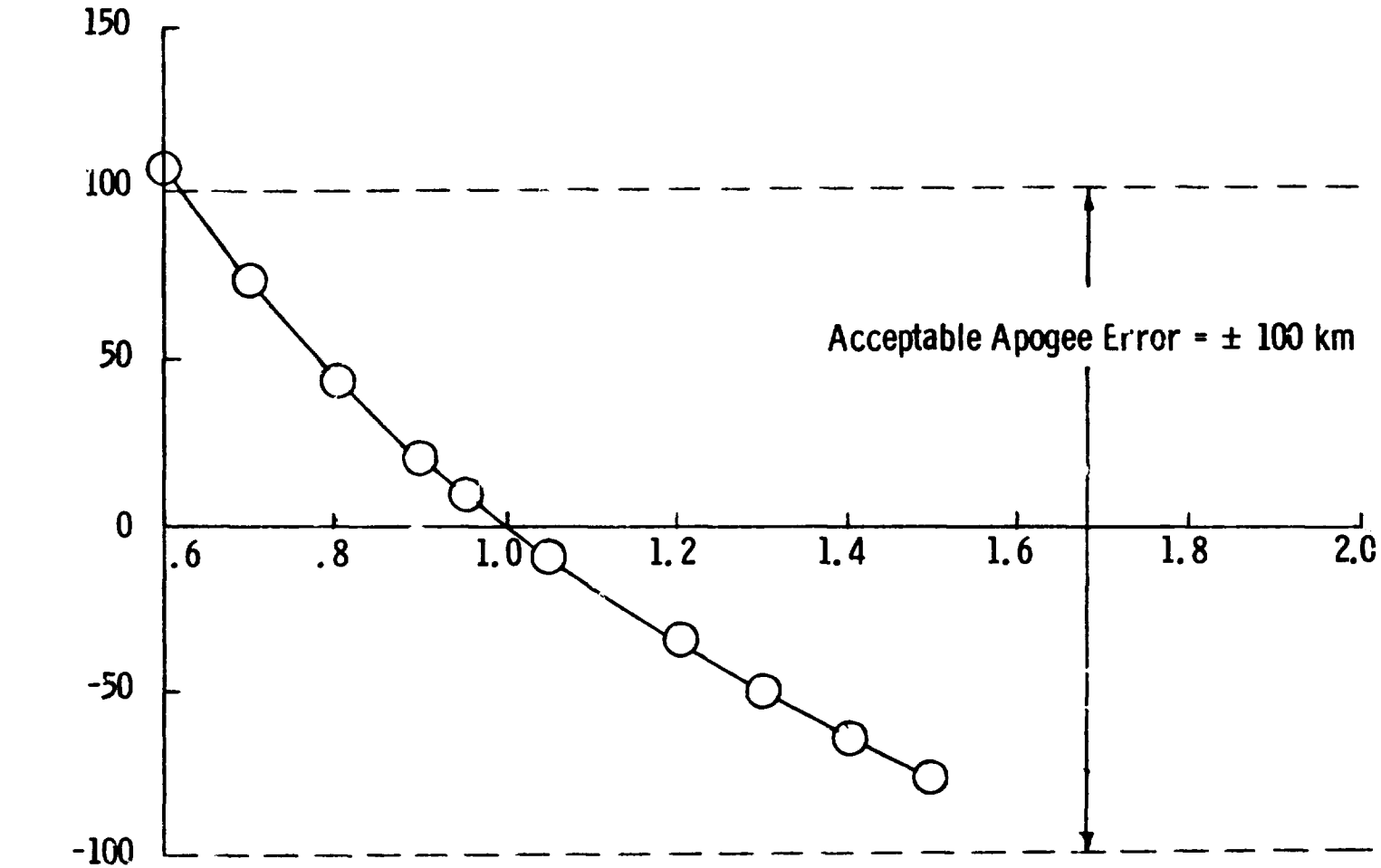

Figure 14. - Apogee error for heuristic linear feedback law test

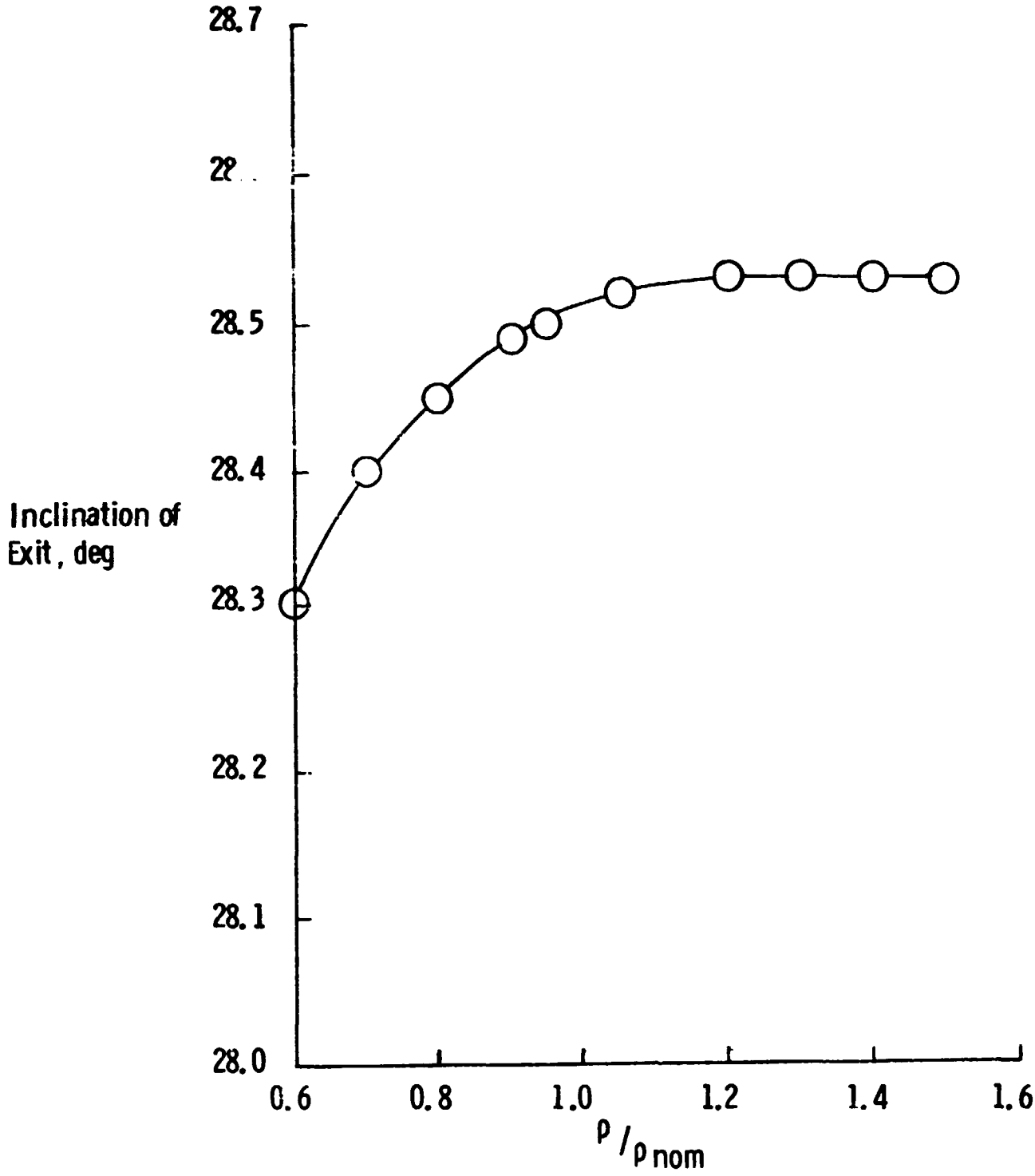

Figure 15. - Variation of final inclination with density factor for the heuristic guidance law

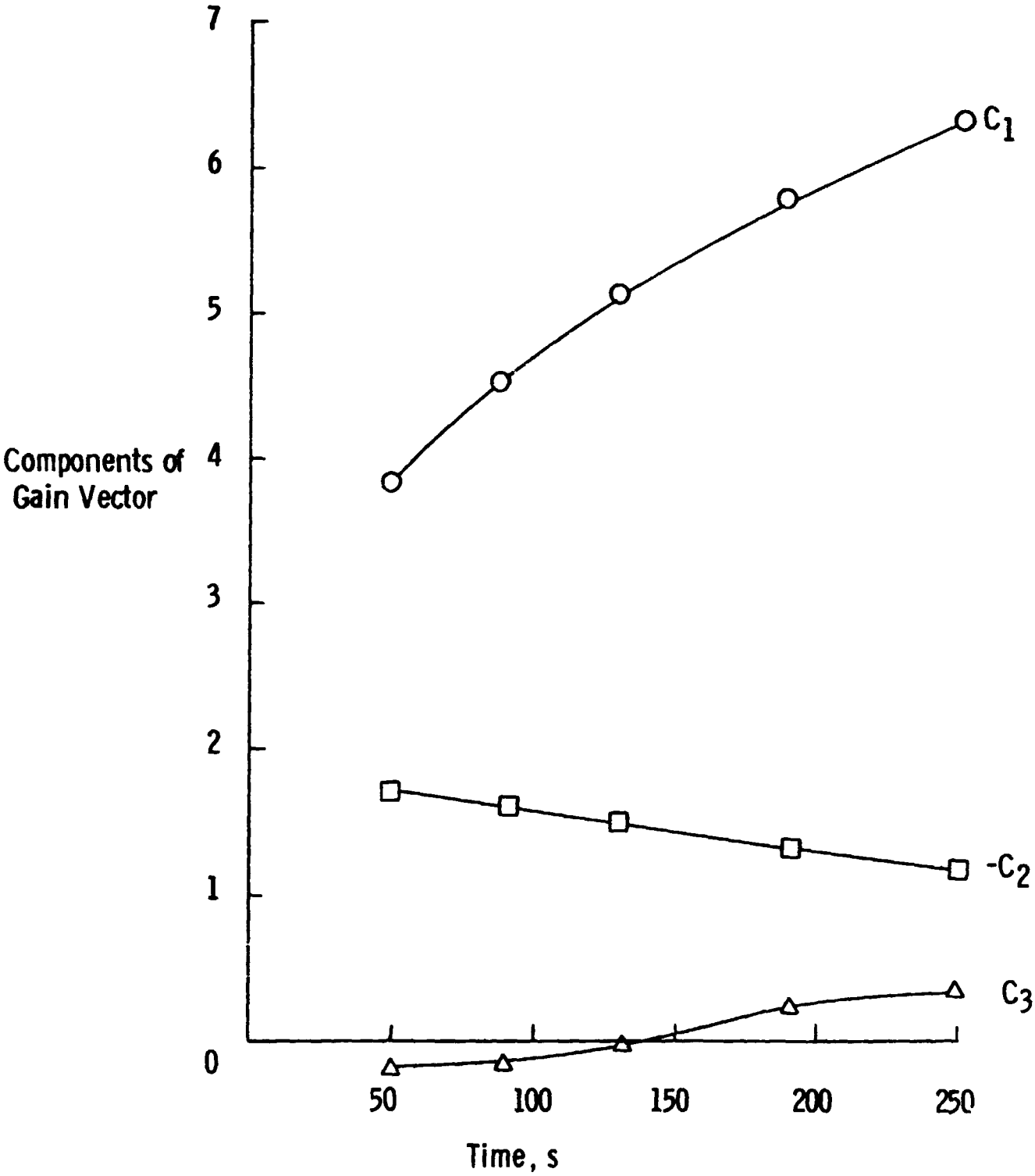

Figure 16. - Gain vector history

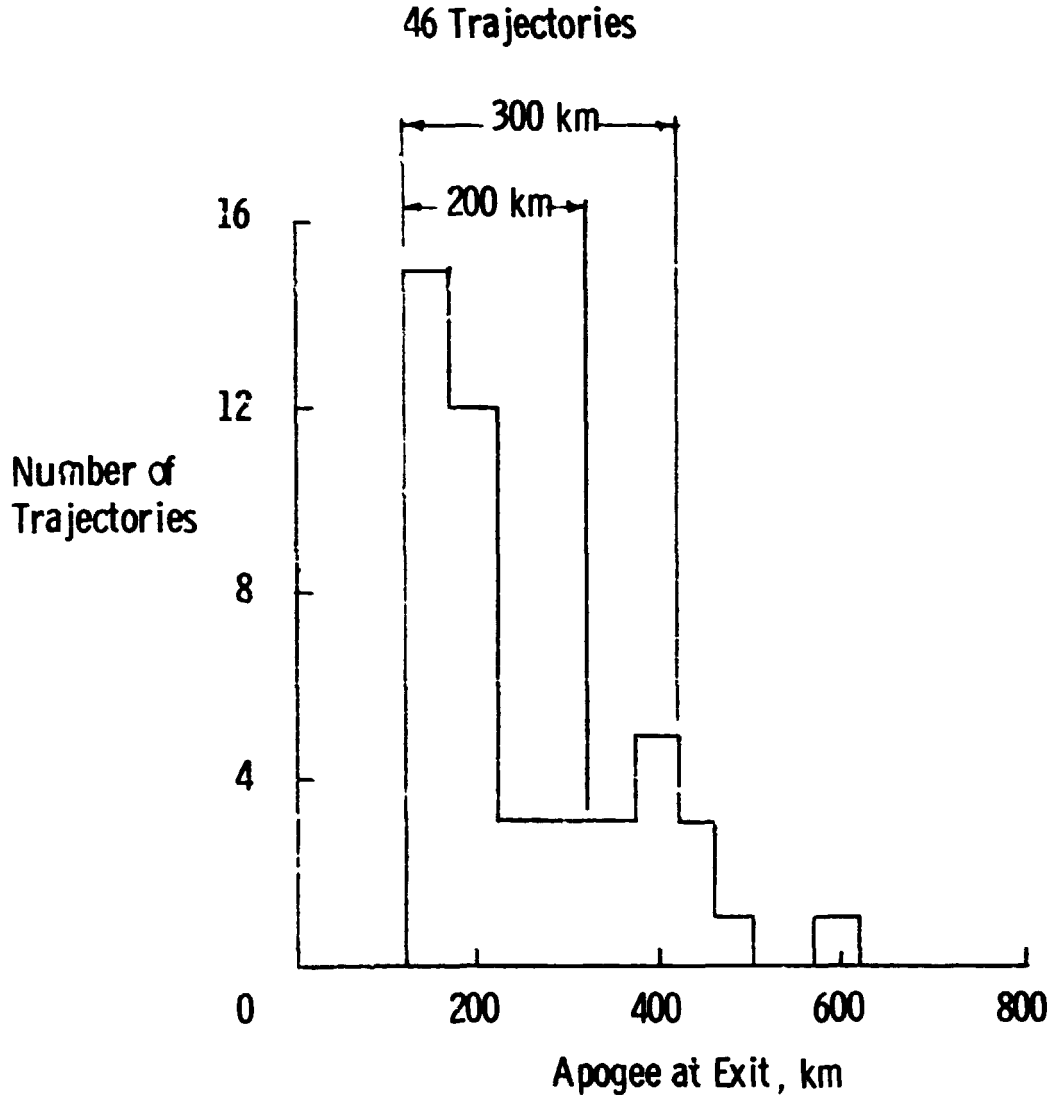

Figure 17. - Histogram of final apogee for optimal regulator test

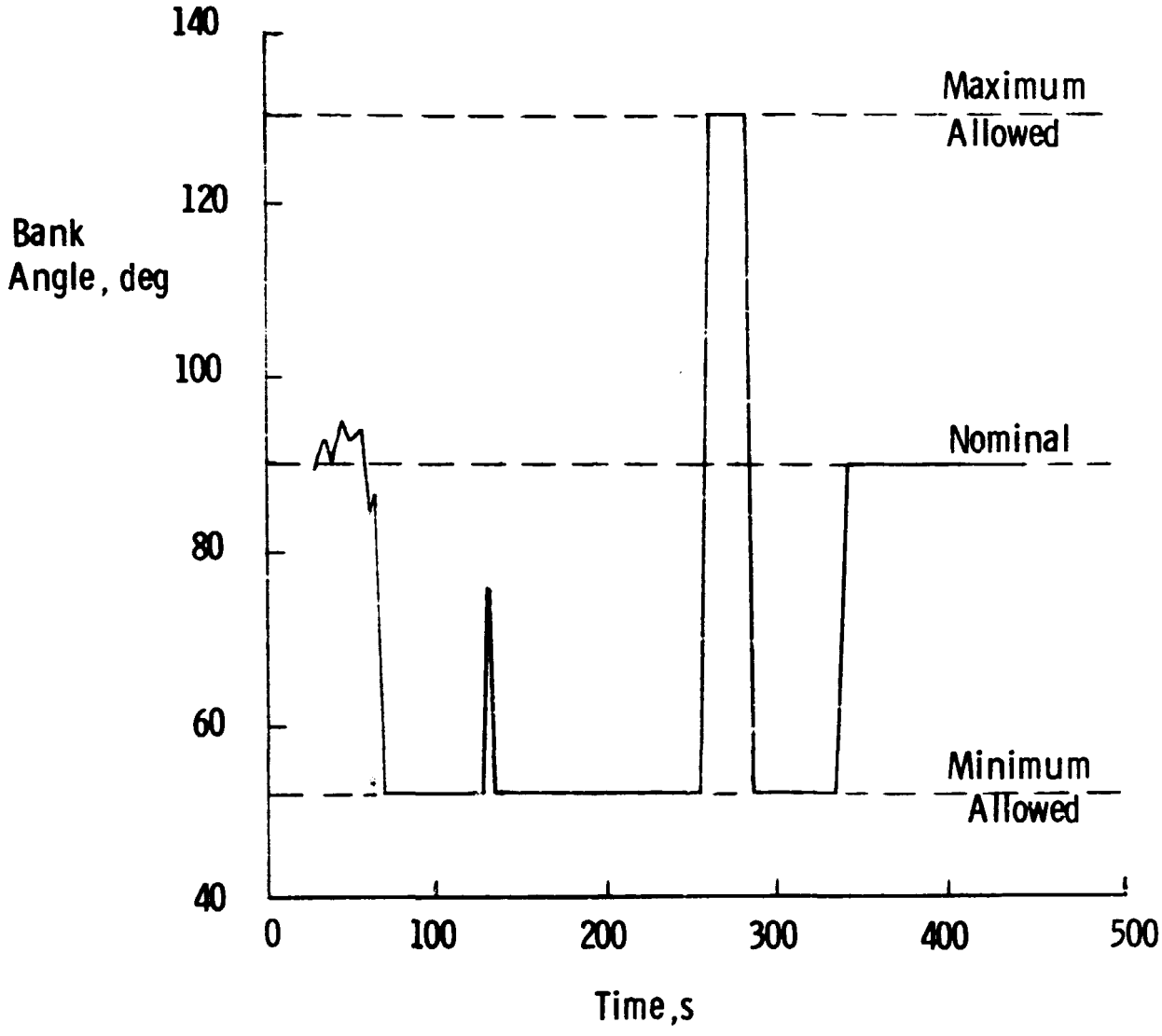

Figure 18. - Typical bank angle history from optimal regulator test